Research Square

Preprints are preliminary reports that have not undergone peer review.
They should not be considered conclusive, used to inform clinical practice,
or referenced by the media as validated information.

Temperature extremes constrain climate-sensitive life traits and reveal genetic correlates of thermal tolerance in the malaria mosquito Anopheles coluzzii

Hassana A. Abdulrahman
Bayero University Kano
Umar Aminu
Bayero University Kano
Hadizat E. Kadir
Bayero University Kano
Muhammad M. Mukhtar
Bayero University Kano
Yusuf Y. Aliyu
Centrum for Tropical and Infectious Diseases Research
Shuaibu Adamu
Centrum for Tropical and Infectious Diseases Research
Abdoul-Nasser H. Sanda
Université André Salifou
Kasim Abdulrahman
Centrum for Tropical and Infectious Diseases Research
Ashiru A. Zainulabidin
Centrum for Tropical and Infectious Diseases Research
Udoka C. Nwangwu
National Arbovirus and Vectors Research Centre
Usman Abdulrasheed
Centrum for Tropical and Infectious Diseases Research
Ibrahim W. Zubair
Federal University Dutse
Musbahu A. Sani
Sa'adatu Rimi University of Education
Isa A. Baba
Bayero University Kano
Charles S. Wondji
Liverpool School of Tropical Medicine

Sulaiman S. Ibrahim

ss.ibrahim@ctidr.org.ng

Bayero University Kano

Research Article

Keywords: Anopheles coluzzii, thermal tolerance, 2La inversion, 1014F, kdr mutation

Posted Date: September 22nd, 2026

DOI: https://doi.org/10.21203/rs.3.rs-10993899/v1

License: This work is licensed under a Creative Commons Attribution 4.0 International License.
Read Full License

Additional Declarations: No competing interests reported.

Temperature extremes constrain climate-sensitive life traits and reveal genetic correlates of thermal tolerance in the malaria mosquito *Anopheles coluzzii*

Hassana A. Abdulrahman[1,2], Umar Aminu[1,2], Hadizat E. Kadir[1,2], Muhammad M. Mukhtar[1,2], Yusuf Y. Aliyu[2], Shuaibu Adamu[2], Ashiru A. Zainulabudin[2], Abdoul-Nasser H. Sanda[2,3], Kasim Abdulrahman[2], Udoka C. Nwangwu[2,4], Usman Abdulrasheed[2], Ibrahim W. Zubair[5], Musbahu A. Sani[6], Isa A. Baba[7,8], Charles S. Wondji[9,10] and Sulaiman S. Ibrahim[1,2,3,4,9]✉

[1] Department of Biochemistry, Bayero University Kano, PMB 3011, Kano, Nigeria
[2] Centrum for Tropical and Infectious Diseases Research, No. 1, Dederi Street, 700241, Kano, Nigeria
[3] Department of Biological Sciences, Université André Salifou, PMB 656, Zinder, Niger Republic.
[4] National Arbovirus and Vectors Research Centre, 4 Park Ln, GRA, 400102, Enugu, Nigeria
[5] Department of Microbiology and Biotechnology, Federal University Dutse, P.M.B. 7156, Dutse, Jigawa, Nigeria
[6] Department of Mathematics, Sa'adatu Rimi University of Education, PMB 3218, Kano, Nigeria
[7] Department of Mathematics, Bayero University Kano, PMB 3011, Kano, Nigeria
[8] Mathematics Research Center, Department of Mathematics, Near East University, Mersin 10, Nicosia 99138, Cyprus
[9] Centre for Research in Infectious Diseases, PO Box 13591, Yaoundé, Cameroon
[10] Vector Biology Department, Liverpool School of Tropical Medicine, Pembroke Place, L3 5QA, United Kingdom

✉ Correspondence: Sulaiman S. Ibrahim: ss.ibrahim@ctidr.org.ng

Abstract

Background: Temperature shifts associated with climate change are reshaping mosquito distributions, fitness-related life-history traits and pathogen transmission potential. While moderate warming may enhance survival, development and reproduction, thermal extremes may constrain fitness and vectorial capacity. Predicting temperature effects on *Anopheles* population dynamics is essential for evidence-based vector control and malaria risk management in the future warmer world.

Methods: We investigated discrete, acute temperature exposures on survival and development of immature stages of the field-derived malaria mosquito *Anopheles coluzzii.* Eggs, larvae and pupae were exposed for 1 h to temperatures ranging from 0 to 43°C. Stage-specific egg hatching, larval mortality, pupation and adult emergence were assessed, together with carry-over effects of larval temperature exposure.

Results: Eggs were more heat- than cold-sensitive, with 23.60°C predicted as the optimum for hatching, a narrow 25–28°C window supporting hatching over time, and 38-39°C as the threshold beyond which hatching ceases. Larval survival was optimal at 24.6°C, with lowest mortality within 25–28°C. Larvae were also more heat- than cold-sensitive; mortality was 55% at 0°C, whereas no larvae survived 43°C. Larval thermal exposure reduced pupation from 85% in controls to 55% at 38°C and 45% at 0°C, with no pupation at 43°C. Adult emergence from exposed larvae declined from 85% in controls to 38% at 42°C. Stage-specific pupal mortality increased from 3% in controls to 52% at 0°C and 100% at 43°C, with 24.41°C predicted as the optimum for survival, and 25–28°C defining the best survivorship window. Emergence from exposed pupae declined from 97% in controls to 48% at 0°C and 60% at 42°C, with optimum of 24.19°C. Genotyping of extreme larval and pupal phenotypes (alive at 41°C

vs dead at 38°C) revealed associations between heat tolerance and the $2L^a$ chromosomal inversion polymorphism and the 1014F *vgsc kdr* mutation.

Conclusion: Beyond 42°C larval and pupal survival ceased, with thermal hierarchy of survival established as pupae > larvae > eggs. These findings demonstrate broad thermal breadth in this species and implicate $2L^a$ and 1014F *kdr* mutation in heat tolerance, providing insight into mechanisms that may shape future population dynamics and malaria transmission risk.

Keywords: *Anopheles coluzzii*, thermal tolerance, $2L^a$ inversion, 1014F, *kdr* mutation

1. Background

Anthropogenic climate change is causing a long-term increase in global mean temperatures, altering regional climate patterns, and inducing extreme weather events (Ranasinghe et al., 2023). These changes include shifts in local and regional temperatures, humidity and precipitation levels, as well as flooding, all of which in turns affect the distribution and population expansion, seasonality, and transmission intensity of human (e.g., malaria) and zoonotic vector-borne diseases (IPCC, 2022; Ranasinghe et al., 2023). Malaria still ravages sub-Saharan Africa, with the continent alone accounting for ~94% of all reported global cases, and 95% of the estimated 610,000 malaria-related deaths in 2024. And Nigeria alone contribute ~24% of all global malaria cases and about one-third of all malaria-related deaths (WHO, 2025).

As global warming scrambles our ecosystems, speeding up proliferation of disease-transmitting insects, additional deaths have been projected from climate impacts on diseases like malaria (IPCC, 2022; WHO, 2023). The mechanistic basis of how mosquitoes will respond and adapt to the rapid anthropogenic climate warming is one of the major ecological concern of public health importance (Couper *et al.*, 2021). Depending on the degree of local warming and the mosquitoes' ecology, it is predicted that distribution of populations may change, with contrasting shifts, expansions or declines (Ren *et al.*, 2016; Couper *et al.*, 2021), resulting in patterns that vary by region (Hoegh-Guldberg *et al.*, 2018). Mechanistic studies which utilize temperature-dependent modelling, e.g., (Ryan, Lippi and Zermoglio, 2020) have predicted a geographic shifts in endemic regions and seasonal suitability for malaria transmission in the future warmer world, with the more mesic/humid regions in East and Southern Africa disproportionately carrying higher burden, compared with the more xeric West Africa.

Temperature constrains the life of malaria mosquitoes, dictating their ectothermic fitness traits. It impacts egg to adult survival, development rates and adult longevity (Oliver and Brooke, 2017, Rebaudo and Rabhi, 2018), modifies biting rate and fecundity, and malaria parasite development rate and vector competence (Paaijmans *et al.*, 2010; Villena *et al.*, 2022). Several studies have documented the impact of thermal extremes on the fitness of mosquitoes. For example, a study which investigated the impact of temperature variations (40-48°C for 10 min) on egg hatching rates in *An. gambiae* s.s. from Kenya (Huang et al., 2006) established 40°C as the maximum tolerable temperature beyond which the rate of egg hatching failure increases linearly. The eggs tolerated brief exposures up to 44°C, with eclosion dropping from >50% at 44°C to about 12% at 45°C, with no eggs hatching at 46°C or higher temperatures. Other studies on *Anopheles* larvae, e.g., (Christiansen-Jucht *et al.*, 2015) have shown that increased rearing temperatures during the larval stages of *An. gambiae s.s.* impacted development rates, inducing reduce body size, leading to smaller adults. For adults, they also showed that starting from 31°C, higher temperatures significantly decreased the probability of blood feeding, reduce fecundity (number of eggs laid), as well as egg hatching (fertility). Another study using *An. coluzzii* and *An. gambiae* s.s. populations from three sites in northern Nigeria, which were exposed to range of temperatures spanning 5 and 46°C has documented a very high thermotolerance, with no mortality in larvae at 38°C, and LT_{50} of ~44°C (Ibrahim *et al.*, 2021). A recently published study has looked into the impact of constant (27°C) and fluctuating (e.g., 27°C ± 3) temperatures on the life traits of lab. colonised *An. coluzzii* (Ngousso) and *An. gambiae* s.s. (Kisumu) (Pazmiño-Betancourth *et al.*, 2026). These authors showed that *An. gambiae* s.s. larvae exhibited higher survival under fluctuating temperature, while *An. coluzzii* larvae survived better under constant temperature, with

this pattern reverse in adulthood, when *An. coluzzii* survived better and possess larger body size under fluctuating temperatures, and pupate faster overall.

However, the majority of these studies capture very narrow temperature ranges, e.g., (Christiansen-Jucht *et al.*, 2015); most of them did not capture cold extremes (IPCC, 2022); and many utilized long colonized laboratory mosquitoes, e.g., (Bayoh and Lindsay, 2003; Pazmiño-Betancourth *et al.*, 2026) which might have lost their genetic variability.

Several trait-based modelling studies, e.g., (Mordecai *et al.*, 2013, 2019) were parameterized using thermal performances generated from lab colonized mosquitoes to predict transmission indices (R_0), but these domesticated mosquitoes may have lost their genetic variability, and may not represent field populations. Also, stage-structured, temperature-dependent malaria models are increasingly used to address the limitations of simple compartmental formulations by explicitly representing mosquito life stages and age classes. For example, Traoré and colleagues (Traoré *et al.*, 2021) developed a temperature-dependent malaria transmission model with a stage-structured mosquito population, showing that periodic, temperature-driven variation in juvenile and adult mosquito densities can generate seasonal malaria outbreaks when forced with monthly mean temperatures from Burkina Faso. But they represented temperature effects through generic periodic functions rather than life-stage-specific thermal performance curves derived from experiments. Another study (Beck-Johnson *et al.*, 2013) built a delayed, temperature-dependent, stage-structured model for *Anopheles* population dynamics and malaria transmission, demonstrating that including the full mosquito life cycle makes vector abundance and the density of potentially infectious adults much more sensitive to temperature than previously appreciated; yet their model relied on composite temperature response functions and did not directly incorporate experimentally measured mortality and development rates for each immature stage. More recently,

148 another study (Petros *et al.*, 2025) proposed a two-class age-structured, temperature-dependent
149 partial differential equation model with optimal control, capturing age heterogeneity and fitting
150 temperature-dependent transmission to *Plasmodium* infection prevalence data, but this study
151 treated temperature via fitted functions at the population level rather than parameterising each
152 ontogenetic transition with laboratory-derived thermal traits.
153 As ectotherms, mosquitoes are sensitive to even small temperature fluctuations, including
154 alteration in the amplitude and frequency of diel temperature variations, associated with the
155 changing climate (Colinet *et al.*, 2015), which may impose consequence on survival and life traits
156 in microenvironment. Heatwaves are projected to become increasingly frequent and intense and
157 expected to exert significant ecological pressure on ectothermic organisms, pushing them closer
158 to their upper thermal limits (IPCC, 2022; Kramer *et al.*, 2026). Mosquitoes, like other insects
159 utilize several mechanisms to persist, including geographic range shifts to pursue optimal thermal
160 conditions, alterations in daily and/or seasonal behavioral patterns to evade elevated temperatures,
161 behavioral thermoregulation (i.e., the active pursuit of cooler microhabitats/refugia), and enhanced
162 thermal tolerance as a consequence of genetic/evolutionary adaptations (Pu, Wang and Chung,
163 2020; Couper *et al.*, 2021, 2024; Ibrahim *et al.*, 2021). Among the adaptive/genetic mechanisms
164 chromosomal inversion polymorphisms, especially the $2L^a$ inversion in *An. gambiae* s.l. (Coluzzi
165 *et al.*, 1979; Ayala, Ullastres and González, 2014), stands out, as they are maintained in spatially
166 and temporally heterogenous environment and segregate along climatic gradients of aridity
167 (Coluzzi *et al.*, 1979; Wondji *et al.*, 2005). The frequencies of the chromosomal inversion
168 polymorphism, e.g., the $2L^a$, is known to be strongly and significantly correlated with a number of
169 adaptive, phenotypic traits in the *Anopheles,* including insecticide resistance, thermal tolerance,
170 behavioral plasticity and *Plasmodium* susceptibility, desiccation resistance, etc. (Brooke, Hunt and

Coetzee, 2000; Gray *et al.*, 2009; Rocca *et al.*, 2009; Fouet *et al.*, 2012; Riehle *et al.*, 2017; Ibrahim *et al.*, 2021). Unfortunately, the majority of the studies that investigated the role of structural changes on thermal tolerance have also utilized laboratory colonized populations.

Other adaptive, genomic changes, which may be linked to thermal tolerance include the target site insensitivity mutations, e.g., the knockdown resistance [*kdr*-west (L1014F) and *kdr*-east (L1014S)] (Martinez-Torres et al. 1998; Ranson et al. 2000) in the voltage-gated sodium channel (*vgsc*) gene, which reduce binding of pyrethroids and DDT in *Anopheles*; which have also been linked to male mating competitiveness (L1014/1014F heterozygote) genotype (Platt et al. 2015), as well as to blood feeding successes rates in resistant *Anopheles* mosquitoes (Diop et al. 2021). Despite this, prior to this, there were no studies which investigated the pleiotropic effect of the *kdr* mutations on *Anopheles* thermal tolerance have not been conducted.

To predict the potential ecological consequences of sudden diel temperature shifts outside permissive thermal ranges, we experimentally quantified the thermal performance of aquatic life stages of the major malaria vector *An. coluzzii* using discrete, static exposures across a range of temperatures. Specifically, we measured the effects of temperature on egg hatching rate, and stage-specific larval and pupal mortality, as well as developmental speed, expressed as larval pupation rates and pupal emergence rates to adults. We also documented the carry-over effect of the different temperatures on the development rate of larvae through pupae, to emergence. The resulting phenotype data were used to parameterize the temperature dependence of each immature transition explicitly, enabling us to link experimentally observed thermal limits and optima at successive life stages to emergent vector population dynamics. We then used alive and dead larvae and pupae to investigate the role of the $2L^{a}$ chromosomal inversion polymorphism and the 1014F *kdr* mutation on heat tolerance.

2. Methods

2.1 Collection of mosquitoes and identification to species level

Larvae of *An. coluzzii* were collected from rice paddies, in irrigation sites in Auyo town (12°21′N, 9°59′E), Jigawa state, Nigeria, between the months of June, July, and August in 2025. Details of this site was provided in a previous publication (Ibrahim *et al.*, 2014). The larvae were collected using dippers, sieved in each occasion and transferred to the CTID^{R} insectary. Larvae were maintained in insectary conditions of 25°C, ~75–80% humidity, and, 12h:12h day:night cycle, and fed with Tetramin baby fish food. The F_0 adults were fed 10% sucrose solution, randomly mixed, and 4-5 d old females were offered blood. Gravid females were allowed to lay eggs freely in oviposition bowls lined filled with water and lined with filter papers.

For each collection a subset of F_0 females were randomly selected ($n \geq 32$), morphologically identified using according to taxonomic keys (Coetzee, 2020), and following oviposition, identified to species level using PCR. A total of 16 randomly selected F_0 females from the above females were homogenized, genomic DNA (gDNA) extracted using LIVAK protocol (Livak, 1984), and used for SINE200 PCR (Santolamazza *et al.*, 2008).

2.2 Investigation of the impact of temperature on egg hatching

To identify critically permissive temperatures for egg hatching, a total of 840 F_1 eggs were split into fourteen batches, one batch was used as control (60 eggs) and the rest (13 batches) as experimental cohort. For each test temperature, 60 eggs were used, as 6 replicates of 10 eggs placed into PCR strips containing 100 µL of deionized water. The strips were thermocycled for 1 h at 0, 10, 15, 28, 30, 32, 34, 36, 38, 40, 41, 42, and 43°C, following a previous protocol (Huang *et al.*, 2006). For control, 6 replicates of 10 eggs were also transferred into PCR strips containing 100 µL

of deionized water, but were kept at room temperature (25ºC). Following each treatment eggs were placed in separate paper cups with 200 mL of water, the cup covered with nets and a rubber band, and the number of eggs that hatched were recorded every 24 h for 7 d.

2.3 Investigation of stage-specific impact of temperature on larvae, and its carry-over effects on pupation and adult emergence

To investigate if a single heat or cold exposure can impact the fitness of *An. coluzzii*, batches of third-fourth instar F_1 larvae (540 in total, and not heated at egg stage) were split into eight groups of 60 larvae each, and exposed to acute thermal challenges across temperature gradients. From each experimental group 6 replicates of 10 larvae were transferred into 25 mL tubes containing 7 mL of deionized water and placed in a circulating water bath, Grant Optima TXF200 (Grant Instruments, Cambridge, UK), pre-set to 0, 10, 15, 38, 40, 41, 42, and 43°C for 1 h, following previously described protocols (Bayoh and Lindsay, 2003; Ibrahim *et al.*, 2021). Following treatment, the larvae were transferred into paper cups containing 200 mL deionized water covered with nets, and supplied with Tetramin baby fish food. Additional 60 larvae were used as control (exposure at 25°C only). The larvae were maintained in standard insectary condition above, and immediate larval mortality (1 h), delayed mortality (24 h) were recorded. In addition, to investigate if heat preselection at larval stage impact downstream development rate, pupation rate, and adult emergence rates were recorded for 8 d, until all larvae had either developed to adults or died.

2.4 Investigation of stage-specific impact of temperature on pupae, and its carry-over effects on adult emergence

Batches of F_1 pupae (480 in total, and not heated at egg and at larval stage) were split into eight groups of 60 pupae each for experimental cohort (7 replicates), while 60 pupae were used as control. From each experimental group 6 replicates of 10 pupae were transferred into 25 mL tubes containing 7 mL of deionized water and placed in a circulating water bath (Grant TXF200) pre-set to 0, 15, 38, 40, 41, 42, and 43°C for 1 h (Bayoh and Lindsay, 2003; Ibrahim *et al.*, 2021). The control pupae were transferred into six unheated tubes containing 7 mL deionized water, and kept at room temperature (25°C). Following treatment, the pupae were transferred into bowls containing 200 mL deionized water covered with nets, maintained in standard insectary condition above, and immediate mortality (1 h) and delayed mortality (24 h), and adult emergence rates were recorded for 3 d, until all pupae had either emerged to adults or died.

2.5 Temperature-dependent stage-structured *An. coluzzii* population dynamic modelling

To translate the experimental thermal performance data (Sections 2.2–2.4) into a predictive mosquito population dynamic, we developed a temperature dependent stage structured mathematical model for the immature stages of *An. coluzzii* (Arifin *et al.*, 2014; Roux *et al.*, 2015). The model considers three independent life stages: Egg (E(t)), Larva (L(t)), and Pupa (P(t)). In line with the experimental design, where each stage was exposed separately to a thermal challenge without transitions between stages, the model assumes no transitions between compartments. Instead, each stage receives its own constant recruitment rate (the initial cohort size, e.g., 60 individuals per treatment), and temperature acts independently on development and mortality within each stage.

The dynamics of the stage specific populations were presumed to be governed by the following system of ordinary differential equations:

$$\frac{d\mathrm{E(t)}}{dt} = \Lambda_E - \beta_{\mathrm{E}}(\mathrm{T})\mathrm{E(t)} - \mu_E(\mathrm{T})\mathrm{E(t)},$$

$$\frac{d\mathrm{P(t)}}{dt} = \Lambda_P - \beta_{\mathrm{P}}(\mathrm{T})\mathrm{P(t)} - \mu_P(\mathrm{T})\mathrm{P(t)},$$

$$\frac{d\mathrm{L(t)}}{dt} = \Lambda_L - \beta_{\mathrm{L}}(\mathrm{T})\mathrm{L(t)} - \mu_L(\mathrm{T})\mathrm{L(t)},$$

Where:

$\mathrm{E(t)}, \mathrm{L(t)}, \mathrm{P(t)}$: are the numbers of eggs, larvae, and pupae at time t ;

$\Lambda_E, \Lambda_L, \Lambda_P$: are the constant recruitment rates;

$\beta_{\mathrm{E}}(\mathrm{T}), \beta_{\mathrm{L}}(\mathrm{T}), \beta_{\mathrm{P}}(\mathrm{T})$: are the temperature dependent development rates (hatching rate (eggs), pupation rate (larvae), and emergence rate (pupae);

$\mu_P(\mathrm{T}), \mu_L(\mathrm{T}), \mu_P(\mathrm{T})$ are the temperature dependent mortality rates (hatching failure, larval mortality, pupal mortality);

T denotes temperature in ^{o}C.

All temperature dependent parameters were estimated directly from the experimental data described in Sections 2.2–2.4, using the observed rates at each temperature (0, 10, 15, 25, 28, 30, 32, 34, 36, 38, 40, 41, 42, 43^{o}C) for eggs. For larvae, responses to additional temperatures: 28, 30, 32, 34 and 36^{o}C were interpolated from patterns in responses to the experimentally tested temperatures (0, 10, 15, 25, 38, 40, 41, 42 and 43^{o}C) (**Additional file 1**). Similar approach was used for pupae, which were experimentally tested at 0, 15, 25, 38, 40, 41, 42 and 43^{o}C, while responses to 10, 28, 30, 32, 34 and 36^{o}C were interpolated.

2.6 Investigation of the role of the 2La chromosomal inversion on thermal tolerance

To investigate the role of the 2La chromosomal inversion polymorphism on the ability of larvae and pupae to survive high temperatures additional experiments were carried out with these immature stages, exposing them (as done above) to 38°C and 41°C. Larvae with contrasting phenotypes, e.g., alive at 41ºC (highly thermotolerant, T_t, n = 50) and dead at 38°C (relatively thermosensitive, T_s, n = 50) were used for gDNA extraction and genotyping. In addition, this approach was utilized to genotype pupae that died at 38ºC (n = 10) and those that survived at 41ºC (n = 17). Genotyping was conducted utilizing primers and protocols described in previous publication (White *et al.*, 2007). These three set of primers were the Universal reverse, 23A2: (CTCGAAGGGACAGCGAATTA, the 27A2, for 2La: ACACATGCTCCTTGTGAACG, and DPCross5, for $2L+^a$: GGTATTTCTGGTCACTCTGTTGG. The PCR mix comprised 6.42 µL of ddH_20, 1.5 µL of 10× Buffer A, 0.7 µL of 25mM of ($MgCl_2$), 0.25 µL of 2.5mM deoxynucleotide triphosphate (dNTP) mix, 0.5 µL of each of the aforementioned three primers at a concentration of 1 µM, and 0.13 U/µL of KappaTaq DNA polymerase (KAPA Biosystems, Wilmington, MA, USA). Thermocycling condition was 94°C for 3 min, followed by 35 cycles each comprising 94°C for 30s, 60°C for 30 s, and 72°C for 45 s; with final extension at 72°C for 10 min. The PCR amplicons were resolved on a 2% agarose gel, stained with pEqGREEN, and bands visualised. Bands corresponding to 2La and $2L+^a$ configurations were determined to be 492 bp and 207 bp, respectively, with heterozygous mosquitoes exhibiting both bands. Positive controls gDNA of homozygous inverted, heterozygous inverted and standard un-inverted were included in the PCR run.

2.7 Investigation of the role of the L1014F *kdr* mutation in thermotolerance

To detect whether the 1014F *kdr* mutation is also linked with thermal tolerance, the above larvae which exhibited contrasting phenotypes, e.g., alive at 41°C (n = 50) and dead at 38°C (n = 50) were genotyped. Genotyping was conducted using primers and the protocol of (Martinez-Torres *et al.*, 1998). Amplification was carried out with the following primers: Agd1 (ATAGATTCCCCGACCATG), Agd2 (AGACAAGGATGATGAACC), Agd3 (AATTTGCATTACTTACGACA), and Agd4 (CTGTAGTGATAGGAAATTTA). The PCR mix comprised 6.5 µl of HS^{TM} PCR mix (GDSBio, Guangzhou, Guangdong, China), containing optimized concentrations of $MgCl_2$ and dNTPs, 0.5 µl each of the above four primers, to which 1.75 µl of ddH_2O and 2.5 µl of gDNA was added to make a total volume of 12.5 µl. Thermocycling conditions were initial denaturation at 95°C for 3 min, followed by forty cycles each of 94°C for 1 min, 48°C for 2 min, and 72°C for 2 min; followed by a final extension step at 72°C for 10 min. Amplified fragments were separated on a 2% agarose gel, stained with pEqGREEN and visualised. Bands corresponding to the resistant (1014F/F), and susceptible (L/L1014) genotypes were 195 bp and 137 bp, respectively, with a control band at 293 bp. Heterozygote larvae exhibited all three bands. Genomic DNA from known positive samples for these contrasting genotypes were used as control.

2.8 Data Analysis

Statistical analyses were conducted with Python (version 3.14), using an independent student's t-test. To illustrate the effect of temperature on performance traits (egg hatching, mortality, pupation, and emergence) thermal performance curves were created using Python (version 3.1) scipy.optimize.curve_fit package, predicting the temperature minima, temperature maxima, and optimal temperatures. Thermal limits (lower and upper LT_{50}) were estimated using R MASS,

package (version 4.4.3). Kaplan-Meier survival analysis and cumulative incidence curve were performed using the Python package lifelines.KaplanMeierFitter and lifelines.statistics.logrank_test.

The mathematical model was parameterized using the experimentally generated temperature-dependent development and mortality data for each immature stage (egg, larva, and pupa). Dynamical simulations were performed by numerically solving the governing differential equations across the experimental temperature range. Model outputs were analysed using numerical and graphical approaches, including thermal response curves, equilibrium analysis, net population change across temperature gradients, temporal heatmaps of development and mortality, and failure-to-success ratios. The model simulations were performed in Python using the SciPy library for numerical integration of the dynamical system and Matplotlib/Seaborn for visualization of the thermal response surfaces and heatmaps.

To establish a correlation between thermotolerance and the $2L^a$ inversion (categorical variables), odds ratio and a chi-square test of independence was conducted on Python using (statsmodels.stats.contingency_tables.Table2x2 package). In order to determine the correlation between phenotype and genotype, phenotypic data from the thermal assay and the $2L^a$ genotyping data from both larvae and pupae were subjected to multiple correspondence analyses using the R environment (version 4.4.3) packages FactoMineR (for analysis) and factoextra (ggplot2-based visualization). Similar approaches were utilized for the analysis of 1014F *kdr* mutation analysis.

3. Results

3.1. Molecular Identification of *An. coluzzii*

All the 16 F_0 females randomly selected for PCR from each collection spanning three months were *An. coluzzii*, with characteristic bands of ~479 bp (**Figure S1**). Neither *An. gambiae s.s.* and nor *An. arabiensis* were detected.

3.2 Temperature extremes reduce egg hatching

To predict the impact of temperature stress on egg hatching a total of 840 eggs (6 replicates of 10 eggs for each test temperature) were exposed for 1 h to temperatures spanning 0 to 43°C, and hatching rates per temperature were recorded per day for 7 d.

Temperature significantly impacts hatching (**Figure 1a**), with the highest hatching success observed from the control (25°C) eggs (mean hatching rate = ~80%±1.26). At 28°C, hatching rate reduced considerably, but not significantly to ~53%±2.88 ($p = 0.064$, $df = 10.0$, $t = -2.08$). Colder temperatures significantly reduced hatching, from ~80%±1.26 observe in control, to 32%±1.94 ($p<0.001$, $df = 10.0$, $t = -5.11$), 25%±0.84 ($p<0.001$, $df = 10.0$, $t = -8.88$), and 13%±0.82 ($p<0.001$, d f=10.0, t=-10.8) for 15°C, 10°C and 0°C, respectively. High temperatures impacted hatching success negatively. For example, the hatching rates significantly reduced to 27%±1.21 ($p<0.001$, $df = 10.0$, $t = -7.46$), 20%±0.63 ($p<0.001$, $df = 10.0$, $t = -10.4$), 18%±0.75 ($p<0.001$, $df = 10.0$, $t = -10.3$), 12%±0.41 ($p<0.001$, $df = 6.03$, $t = -12.6$), 8%±0.75 ($p<0.001$, $df = 10.0$, $t = -11.9$), and 3%±0.52 ($p<0.001$, $df = 10.0$, $t = -13.7$) at 30, 32, 34, 36, 38 and 40°C, respectively. No eggs hatched at 41, 42, and 43°C, respectively. The optimal temperature (T_{opt}) which support the highest hatching rate was predicted to be ~23.60°C, while -1.96°C (extrapolated) and 41°C were predicted to be the minimum temperature (HT_{min}) and maximum temperature (HT_{max}) which marginally

support hatching, respectively. The lower (LLT_{50}) and upper (ULT_{50}) lethal temperatures, e.g., the low and high temperatures at which 50% of the eggs failed to hatch was predicted as 17.39°C and 28.38°C, respectively.

Modelling egg hatching data clearly delineate three thermal zones: cold stress, optimal range, and heat stress (**Figure 1b**). Positive net change (population growth) was predicted within a defined optimal temperature ranges (~22–28°C), where the net change exceeds 20%. At temperatures below 15°C net change becomes increasingly negative, indicating cold stress and population decline. Similarly, temperatures above 30°C leads to progressive heat stress, with net change dropping below –40% beyond 30°C.

To assess the combined effect of temperature and time on egg hatchability, hatching rates were analyzed across temperature treatments and observation times from 24 to 168 h (**Figure 1c**). Highest hatching was observed at 25°C after 24 h, where 43.3% of eggs hatched. In contrast, temperatures at or below 10°C resulted in consistently low hatching rate, and above 38°C resulted in almost no hatching at all, indicating strong thermal inhibition of egg hatchability. Overall, the heatmap revealed a narrow optimal temperature window between approximately 25 and 28°C, with hatching success varying over time. Improved hatching with time is mainly observed within the optimal, moderate temperature ranges (25-30°C), whereas extremely low and high temperatures remained unsuitable regardless of duration eggs were kept floated in water.

3.3 Temperature extremes impact larval survival and induce carryover effect on pupation and adult emergence

To assess the impact of temperature extremes on larval survival, 540 third-instar F_1 larvae were split up into eight groups, each of which had 60 larvae. Six replicates of 10 larvae each were

exposed to experimental temperatures of 0, 10, 15, 38, 40, 41, 42, and 43°C for 1 h. Immediate (1 h) and delayed mortality (24 h) were recorded, and the larvae were followed documenting the impact of the stage-specific thermal stress rate on their pupation and emergence rates.

3.3.1 Temperature extremes reduce larval survival

Temperature extremes impact larval survival, with the control larvae exhibiting the lowest mean mortality of ~15%±0.84 (**Figure 2a**). Low temperatures, 15°C, 10°C, and 0°C significantly increased mortality, from ~15% in control to ~33%±1.21 ($p = 0.012$, $df = 10.0$, $t = -3.05$), ~47%±1.63 ($p = 0.002$, $df = 10.0$, $t = -4.23$), and ~55%±2.51 ($p = 0.004$, $df = 10.0$, $t = 3.70$), respectively. Similar pattern was observed with high temperatures, 38, 40, 41, 42, and 43°C, increasing larval mortality to ~42%±1.17 ($p = 0.001$, $df = 10.0$, $t = -4.54$), ~40%±1.26 ($p = 0.002$, $df = 10.0$, $t = -4.04$), ~40%±1.67 ($p = 0.008$, $df = 10.0$, $t = -3.27$), ~52%±1.33 ($p<0.001$, $df = 10.0$, $t = 5.72$), and ~100%±0.00 ($p = 0.002$, $t = 0.00$), respectively. Optimal temperature for survival was predicted to be ~24.60°C (**Figure 2a**). The lower most lethal temperature (LLT) and the upper most lethal temperature (ULT) were predicted as -5.59°C (extrapolated) and 43°C, respectively. The lower and upper lethal temperatures (LT_{50}s), which kills 50% of the larvae were estimated to be 8.64°C and 41.86°C, respectively.

To assess the combined effect of temperatures and time on larvae, mortality rates were compared across temperature treatments and observation times from 24 to up to 192 h (**Figure 2b**). Extreme temperatures inflicted highest mortalities within the first 24 h period, with the lowest overall mortality recorded at 25–28°C, and also generally at early time points (24–72 h), defining a thermal temperature vs time window for larval survival.

Kaplan-Meier analysis indicated that larval survival significantly decreased over time under all temperature treatments, compared to controls (**Figure S2**). Survival probabilities beginning at 1.0 (100%) dropped rapidly after 24 h, to 0.0 at 43°C and 0.38 at 0°C, while the control group at 25°C had a survival probability of 0.9. For example, at 41°C, the survival probability sharply decreased from 0.82 at 24 h to nearly 0.2 by 192 h, indicating increased mortality with time. In contrast, the control group maintained a high survival probability of 0.84 throughout the 192 h period. Log-rank test confirmed the statistical significance of the difference in survival rates between the two temperatures ($p = 0.0036$). A similar pattern was observed where survival probabilities declined at various extreme temperatures, with statistically significant differences, at 43°C ($p<0.0001$), 42°C ($p = 0.0055$), 41°C ($p = 0.0037$), 40°C ($p = 0.0027$), 38°C ($p = 0.040$), 10°C ($p = 0.0358$), and 0°C ($p<0.0001$) compared to the control larvae.

3.3.2 Temperature extremes induce carryover reduction in larval pupation

Temperature exposure at larval stage elicits moderate but significant carry-over effect on larval pupation. While mean pupation rates was predicted to be ~85%±0.84 for control larvae (**Figure 2c**), high extremes of 38, 40, 41 and 42°C led to significant decline in pupation, in ranges of ~58%±1.17 ($p = 0.001$, $df = 10.0$, $t = -4.54$), ~60%±1.26 ($p<0.001$, $df = 10.0$, $t = -5.68$), ~60%±1.67 ($p<0.001$, $df = 10.0$, $t = -5.72$), and ~48%±1.33 ($p = 0.022$, $df = 10.0$, $t = -2.70$). Similar patterns were observed for cold temperatures, e.g., mean pupation significantly decreased to ~67%±1.21 ($p = 0.012$, $df = 10.0$, $t = -3.05$), ~53%±1.63 ($p = 0.002$, $df = 10.0$, $t = -4.23$), and ~45%±2.51 ($p = 0.004$, $df = 10.0$, $t = -3.70$), at 15°C, 10°C, and 0°C, respectively. The optimal carryover temperature for highest pupation was predicted to be ~24.73°C, while lower (LPT_{min}) and upper (UPT_{max}) were predicted as -5.59°C and 43°C, respectively.

Combined effect of carryover temperature and time on larval development to pupation was compared across temperature treatments and observation times from 24 h to up to 192 h (**Figure 2d**). Pupation peaked between 25-30°C, with broad success with increase in time, spanning up to 96 h, even at extreme temperatures. Indeed, comparison of pupation success rate and larval mortality as function of temperature indicated that the widest gap in favor of pupation occurs between 20 and 35°C, where success exceeds mortality by 30–70% points (**Figure S3a**). Comparison of pupation success and failure confirmed that failure/success ratio reaches a minimum (0.18) at 25–28°C (**Figure S3b**), rises sharply at temperatures above 38°C, and becomes infinite at 43°C, at which no pupation occurs. Cold temperatures (0–15°C) also show elevated ratios (> 0.5).

3.3.3 Temperature extremes induce carry-over reduction in adult emergence

Temperature exposure induced a carry-over effect on emergence rates of pupae raised from heated larvae (**Figure S3c**). Compared to the highest emergence rate of 85%±0.84 obtained in the control, high temperatures of 38, 40, 41 and 42°C significantly reduced emergence rates to ~55%±1.38 ($p = 0.001$, $df = 10.0$, $t = -4.56$), ~50%±2.10 ($p<0.001$, $df = 10.0$, $t = -8.91$), ~40%±1.55 ($p<.001$, $df = 10.0$, $t = -7.28$), and ~38%±1.33 ($p<0.001$, $df = 7.24$, $t = -5.54$), respectively. Similarly, the emergence rates were significantly reduced at colder temperatures to ~53%±1.97 ($p = 0.005$, $df = 10.0$, $t = -3.63$), ~43%±2.34 ($p = 0.002$, $df = 10.0$, $t = -4.11$), and ~30%±1.67 ($p = 0.004$, $t = 0.00$), respectively for 15°C, 10°C, and 0°C. Optimal emergence temperature was predicted to be ~24.47°C, while the lower (LET) and upper (UET) temperatures that inhibit emergence were predicted to be emergence temperatures as -1.64°C and 43°C, respectively. The LET_{50} and UET_{50} were predicted as 13.33°C and 40°C, respectively.

3.4 Stage-specific impact of temperature on pupae, and its carry-over effects on adult emergence

To investigate the impact of temperature shifts on pupal survival and development rate, assays were conducted with pupae generated from previously unexposed larvae. Batches of F_1 pupae (480 in total) were split into eight groups of 60 pupae each and from each group, 6 replicates of 10 pupae were exposed at 0, 15, 38, 40, 41, 42, and 43°C for 1 h. Immediate (1 h) and delayed pupal mortalities (24 h) were recorded, and adult emergence rates were followed until all pupae emerged or died.

3.4.1 Temperature extremes reduce pupal survival

Temperature significantly impact pupal survival (**Figure 3a**). The lowest mortality of ~3%±0.82 was recorded at 25°C (control). Mortalities for pupae heated at high temperatures of 38, 40, 41, 42, and 43°C significantly increased to ~20%±0.63 ($p = 0.012$, $t = 3.00$), ~23%±1.21 ($p = 0.007$, $df = 10.0$, $t = 3.35$), ~25%±1.64 ($p = 0.016$, $df = 10.0$, $t = 2.89$), ~40%±1.79 ($p = 0.001$, $df = 10.0$, $t = 4.57$), and ~100%±0.00 ($p = 0.002$, $t = 0.00$), respectively. Also, low temperatures of 15°C and 0°C increased mortalities significantly, to ~35%±1.05 ($p<0.001$, $df = 10.0$, $t = 5.84$) and ~52%±1.47 ($p<0.001$, $df = 10.0$, $t = 7.03$), respectively. Optimal temperature for pupal survival was predicted to be ~24.41°C; lower (LLT) and upper (ULT) lethal temperatures were predicted as -4.13°C and 43°C, with 1.5°C and 42.17°C respectively predicted to be the lower (LLT_{50}) and upper (ULT_{50}) lethal temperatures that kill 50% of the pupae.

To assess the combined effect of temperature and time on pupae, mortality rates were compared across temperature treatments and observation times from 24 to up to 72 h (**Figure 3b**). Extreme

492 temperatures inflicted highest mortalities within the first 24 h period, with the lowest overall
493 mortality recorded at 25–28°C, and generally within the first 24 h.
494 Pupal survival significantly decreased over time across all temperature treatments, as revealed by
495 Kaplan-Meier analysis (**Figure S4**). Survival probability was initially 1.0 for all groups, but after
496 24 h, it dropped to 0.0 at 43°C and 0.58 at 0°C, indicating sharp declines at both high and low
497 temperature extremes. For 42°C, at 24 h survival steeply dropped to 0.7 at 42°C, and by 48 h
498 survival probability had declined sharply close to 0.0. In contrast, survival probability was much
499 higher at 25°C, with a flatter slope, remaining high with time, >0.9. Log-rank test confirmed that
500 the differences between the control and 42°C exposed pupae was statistically significant
501 ($p<0.0001$). Similar trends of decreasing survival probabilities was observed at temperatures of
502 43°C, 41°C, and 0°C, with significant differences noted through log-rank tests (43°C, $p<0.0001$;
503 41°C, $p = 0.0046$; 15°C, $p = 0.015$; 0°C, $p<0.0001$) compared to the control pupae. In contrast,
504 while survival probabilities at 38°C and 40°C decreased, the log-rank tests indicated no significant
505 differences (38°C, $p = 0.145$; 40°C, $p = 1.0$) between these experimental groups and the control,
506 suggesting that pupae might have higher heat tolerance compared with larvae.
507
508 ***3.4.2 Temperature extremes reduces pupal emergence to adults***
509 Temperature significantly impact pupal emergence, with high temperatures of 38, 40, 41 and 42°C
510 significantly decreasing emergence from 97%±0.82 obtained in control pupae to ~80%±0.63 ($p =$
511 0.012, $t = 3.00$), ~77%±1.21 ($p = 0.007$, $df = 10.0$, $t = -3.35$), ~75%±1.64 ($p = 0.016$, $df = 10.0$, t
512 $= -2.89$) and ~60%±1.79 ($p = 0.001$, $df = 10.0$, $t = -4.57$), respectively (**Figure 3c**). Low
513 temperatures, 15°C and 0°C also significantly affect emergence, with rates of ~65%±1.05
514 ($p<0.001$, $df = 10.0$, $t = -5.84$) and ~48%±1.47 ($p<0.001$, $df = 10.0$, $t = -7.03$), respectively. Optimal

emergence temperature was predicted to be ~24.19°C, with lower (LLT) and upper (ULT) lethal temperatures which inhibit emergence predicted as -4.13°C and 43°C. Temperatures of 1.5°C and 42.17°C, respectively were predicted to be the lower (LLT_{50}) and upper (ULT_{50}) which reduced pupal emergence by 50%.

To assess the combined effect of temperature and time on pupae, adult emergence rates were compared across temperature treatments and observation times from 24 to up to 72 h (**Figure 3d**). Highest emergence rate was observed around the optimal temperatures, but with emergence of up to 60% in pupae which survived 42°C, suggesting that the pupae were very tolerant to temperature extremes. However, the majority of the pupae emerged within the first 48 h period.

Comparison of adult emergence success vs failure revealed a very low failure/success ratio of ≈0.034 at 25°C, confirming that this temperature strongly favours emergence over mortality (**Figure S5a**). At 0 °C, the ratio is ≈1.07 (slightly above 1, indicating mortality exceeding emergence), while at 10–15°C the ratio falls below 1 (0.82 and 0.54, respectively). Above 30°C, the ratio increases linearly but remains below 0.3 until 40°C. At 42°C, the ratio jumps to 0.67, while at 43°C, emergence is zero, making the ratio infinite (annotated). In essence, pupae exhibited a wide thermal breadths (10–42 °C), at which emergence exceeded mortality, broader than the predicted values from larvae. Net population change was predicted to be positive at all temperatures, except for 0°C (-3.4%) and 43°C (–100%) (**Figure S5b**), with three thermal zones are predicted: cold stress (0–15°C), optimal range (20–32°C), and heat stress (35–45°C). A broad net change optimum occurs between 25°C and 41°C, with the highest net change (≈93 %) at 25°C. The net change curve is asymmetrical; net change declines gradually below 15°C, but collapses abruptly above 42°C, indicating that pupae are more sensitive to extreme heat than moderate cold.

3.5 2La chromosomal inversion is associated with larval heat tolerance

To investigate the impact of $2L^a$ inversion on heat tolerance, highly thermotolerant (T_t) larvae (alive at 41°C, n = 50) and relatively thermos-susceptible (T_s) larvae (dead at 38°C, n = 50) were genotyped (gel pictures are provided in **Figure S6**). In addition, this approach was utilized to successfully genotype pupae that died at 38°C (n = 10) and those that survived at 41°C (n = 17), successfully (gel pictures in **Figure S7**).

The thermotolerant larvae, alive after 41°C heating exhibited disproportionate frequencies of the $2L^a$ inversion alleles (85%), with 39 (~78.0%) larvae bearing homozygote inverted arrangement ($2L^a/2L^a$), 7 (~14.0%) larvae being heterozygotes ($2L^a/2L^{+a}$), while only 4 (~8.0%) larvae harbor the standard, un-inverted arrangement ($2L^{+a}/2L^{+a}$) (**Table 1**). Conversely, a significant majority of the heat-sensitive larvae, which died at 38°C, carried standard arrangement (26, ~52.0% = $2L^{+a}/2L^{+a}$). The rest of these larvae harbour $2L^a/2L^a$ (15, ~30.0%) and $2L^a/2L^{+a}$ (9, ~18.0%) inversion genotypes, corresponding to 48% frequency and 39% allele frequencies.

A statistically significant correlation was observed between heat tolerance and the $2L^a$ inversion [odds ratio = 12.5 (95% CI: 3.9–39.8, $\chi2 = 23$, $p < 0.001$, df = 1)], when comparing the homozygote and heterozygote inverted larvae with the larvae carrying standard arrangements (**Table 1**). Similar significant heat tolerance association was observed when comparing either the homozygote inverted genotypes [odds ratio = 16.9 (95% CI: 5.04–56.6, $\chi2 = 26.8$, $p < 0.001$, df = 1)] or the heterozygote inverted genotypes [odds ratio = 5.06 (95% CI: 1.19–21.4, $\chi2 = 5.31$, $p = 0.032$, df = 1)] to the standard arrangements.

Table 1: Correlation between larval 2La inversion genotypes and heat tolerance.

Population	Phenotype	n	2L^a Alleles			% 2L^a frequency	2L^a allele
			2L^a/2L^a	2L^a/2L^{+a}	2L^{+a}/2L^{+a}	2L^a/2L^a + 2L^a/2^{+a}	
Auyo	Alive	50	39 (~78.0%)	7 (~14.0%)	4 (~8.0%)	46 (~92.0%)	0.85
	Dead	50	15 (~30.0%)	9 (~18.0%)	26 (~52.0%)	24 (~48.0%)	0.39
Total		100	54 (~54.0%)	16 (~16.0%)	30 (~30.0%)	70 (~70.0%)	

Genotypes	Odds Ratio (95% CI)	χ^2 (p value)
2L^a/2L^a + 2L^a/2L^{+a} vs 2L^{+a}/2L^{+a}	12.5 (3.9–39.8)	23 (<0.001)
2L^a/2L^{+a} vs 2L^{+a}/2L^{+a}	16.9 (5.04–56.6)	26.8 (<0.001)
2L^a/2L^a vs 2L^{+a}/2L^{+a}	5.06 (1.19–21.4)	5.31 (0.032)

n = number of successfully genotyped individuals. Numbers in brackets represent percentage frequency. 2L^a/2L^a: homozygote inverted genotype; 2L^a/2L^{+a}: heterozygote inverted genotype; and 2L^{+a}/2L^{+a}: standard un-inverted arrangement.

Multiple correspondence analysis (MCA) identified features explaining the highest variability in the data. The eigenvalues revealed dimensions 1-2 accounting for ~84.0% of the variability in the data (Scree plots are provided in **Figure S8a** showing the contributions of dimensions). Categories of variables with similar profiles clustered closer and together on the factor map. For example, the 2L^a/2L^a genotype was located near the alive category in the negative quadrant of dimension 1, which supports the highest significant association (highest odds ratio) described previously between possession of the 2L^a inversion in the homozygote state and heat survival (**Figure 4a**). Conversely, the 2L^{+a}/2L^{+a} standard arrangement genotype was located on the positive quadrant of dimension 1, close to the variable dead, which is located close to the pole separating dimension 1 from 2. This proximity supports the association between higher heat susceptibility and absence of

the $2L^a$ inversion. The variable $2L^a/2L^{+a}$ contributed the most to the inertia on the factor map (**Figure 4b**).

A total of 27 pupae were genotyped, comprising pupae that died at 38°C (n = 10) and those that survived at 41°C (n = 17) (**Figure S7**). The distribution of $2L^a$ genotype among the 41°C alive pupae was calculate as 6 (~35.3%) $2L^a/2L^a$ homozygotes, 3 (~17.6%) $2L^a/2L^{+a}$ heterozygotes, and 8 (~47.1%) bearing the $2L^{+a}/2L^{+a}$ standard arrangement (**Table S1**), leading to 44% $2L^a$ genotype frequency. Sixty percent (6) of the larvae that died at 38°C carried $2L^{+a}/2L^{+a}$ standard arrangement, 4 (~40.0%) were heterozygotes ($2L^a/2L^{+a}$), while none (0.0%) was homozygote for the inversion ($2L^a/2L^a$), with $2L^a$ genotype frequency established as 20%. Although odds ratios were more than one when comparing homozygote plus heterozygote inversion genotypes to the standard arrangement, and also between homozygote state and standard arrangement, no significant differences were observed. However, this could be due to bias from the lower number of pupae samples utilized compared with the case of the larvae above.

Eigenvalues revealed dimensions 1-2 accounting for ~81.0% of the variability in the data (Scree plots are provided in **Figure S8b**). Categories of variables with similar profiles clustered together on the factor map, e.g., the $2L^a/2L^a$ clustering closer to variable alive, while variable dead clustered closer to the standard arrangement genotype (**Figure 4c**). The variable $2L^{+a}/2L^{+a}$ contributed the most to the inertia on the factor map, followed by $2L^{+a}/2L^{+a}$ (**Figure 4d**).

3.6 1014F *kdr* mutation is associated with larval heat tolerance

Genomic DNA samples extracted from 99 larvae utilized in section 3.5 were used to successfully genotype the 1014F *kdr* mutation (gel pictures are provided in **Figure S9**). This comprises 50 heat-

tolerant larvae (alive at 41°C) and 49 heat-susceptible larvae (dead at 38°C). From the alive larvae, 10 (~20%) were homozygote resistant (RR), the majority, 34 (~68.0%) were heterozygote resistant (RS), and only 6 (~12.0%) carried the homozygote susceptible (SS) genotype (**Table 2**), translating into 54% 1014F *kdr* allele frequency. In contrast, the majority 24 (~49.0%) of the dead larvae were homozygote resistant, few of them were heterozygote (8, ~16.3%), while the rest (17, ~34.7%), were homozygote susceptible. The *kdr* allele frequency was established as 57%.

A statistically significant correlation was observed between heat tolerance and the 1014F *kdr* mutation [odds ratio = 3.9 (95% CI: 1.38–11, $\chi2 = 7.15$, $p = 0.008$, $df = 1$)] when comparing RR + RS genotypes against SS in all alive and dead larvae. A more pronounced association was observed [odds ratio = 12 (95% CI: 3.6–40.3, $\chi2 = 18.9$, $p < 0.001$, $df = 1$) when comparing heterozygote (RS) state against homozygote mosquitoes (SS) larvae. While correlation between homozygote resistant (RR) vs SS was established, it was not statistically significant [odds ratio = 1.18 (95% CI: 0.36–3.87, $\chi2 = 0.78$, $p = 0.75$, $df = 1$)]. Indeed, the high proportion of heterozygote genotype among the alive larvae, coupled with the high proportion of homozygote resistant genotype among the dead larvae, suggests that heat tolerance is associated with 1014F *kdr* heterozygosity.

Table 2: Correlation between 1014F *kdr* genotypes and larval heat tolerance.

Population	Phenotype	n	*kdr* alleles			% *kdr* frequency	*kdr* allele
			RR	RS	SS	RR + RS	
Auyo	Alive	50	10 (~20.0%)	34 (~68.0%)	6 (~12.0%)	44 (~88.0%)	0.54
	Dead	49	24 (~49.0%)	8 (~16.3%)	17 (~34.7%)	32 (~65.3%)	0.57
Total		99	34 (~34.3%)	42 (~42.4%)	23 (~23.2%)	76 (~76.8%)	

Genotypes	Odds Ratio (95% CI)	χ^2 (p value)
RR + RS vs SS	3.9 (1.38–11)	7.15 (0.008)
RS vs SS	12 (3.6–40.3)	18.9 (<0.001)
RR vs SS	1.18 (0.36–3.87)	0.78 (0.75)

n = number of successfully genotyped individuals. Numbers in brackets represent percentage frequency. RR: homozygote resistant alleles; RS: heterozygote alleles; and SS: homozygote susceptible alleles.

Scree plot (**Figure S8c**) depicts the contributions of three dimensions explaining relationship between variables, with dimension 1 accounting for ~50.8% of the total variance, whereas dimension 2 accounts for ~33.3%, which together contribute ~84.1% of the overall inertia for the relationship between the 1014F *kdr* mutation and larval heat tolerance/sensitivity. Categories of variables with similar profiles clustered together on the factor map, with the RS genotype clustering in proximity to the alive variable, supporting the significant correlation already established between heat tolerance and 1014F *kdr* heterozygosity (**Figure 5a**). In contrast, the RR and SS genotypes clustered almost equidistant to the variable dead on dimensions 1 and 2, respectively, suggesting a lack of association between these genotypes and the heat tolerance phenotype.

633 # 4. Discussion

634 ## 4.1 Extreme temperatures constrain egg hatching in *An. coluzzii*

635 Increasing temperature associated with climate change is impacting the distribution and disease
636 transmission capabilities of vectors, including malaria mosquitoes. Forecasting temperature
637 extremes at which different life stages of malaria mosquitoes can survive and reproduce is a pre-
638 requisite for tailored, climate-responsive control measures.

639 In this study, the predicted optimal temperature for egg hatching was ~23.60°C, with experimental
640 and modelling data showing that temperatures within the ranges of 22-28°C are permissible for
641 productive egg hatching and growth, and temperatures below 15°C and above 30°C resulting in
642 significant reduction in hatching rate. Our findings was in line with the report on *An. gambiae s.s*.
643 from Kenya (Huang *et al.*, 2006), in which the upper tolerated temperature was around 40°C, with
644 egg hatching failure increasing linearly with time above this temperature, reaching 100% at 44°C
645 for 30 min; and no egg hatching following 10 min exposure at 45°C. Another study which used
646 laboratory colonized *An. gambiae* s.s. from Kenya (MBITA strain) has established that eggs held
647 at 22 and 27°C had the highest overall mean hatching count, and temperatures of 12 and 42°C
648 significantly reduced mosquito egg viability (Impoinvil *et al.*, 2007). This is similar to our finding
649 of only 3% of eggs hatching at 40°C and no eggs hatching at 41, 42, and 43°C, respectively. Indeed,
650 a foundational study that followed temperature-dependent development rate has established that
651 *An. gambiae* eggs can tolerate temperatures of up to 40°C (Bayoh and Lindsay, 2003). Elsewhere,
652 in *Aedes aegypti* from Bangladesh egg hatching was supported at temperatures up to 37°C, but got
653 abolished at 42°C regardless of exposure time (Anee *et al.*, 2021). As well, 37°C was found to be
654 a threshold temperature that caused a significantly reduced hatching in *Ae. aegypti*, Bora strain,
655 while 40°C abolished it (Sukiato *et al.*, 2019). Temperature effects could be explained by the

physiological stress the eggs undergo, which is thought to interrupt embryogenesis (Sukiato *et al.*, 2019). One mechanism that is likely to explain this pattern of lethality is protein denaturation (Nguyen, Morange and Bensaude, 1989; Huang *et al.*, 2006). Studies on *Drosophila*, e.g., (Kale *et al.*, 2023) have found that subjecting embryos to heat during the initial stages of embryonic development results in an augmented incidence of embryonic lethality.

4.2 Temperature extremes reduce larval survival and its developmental rate to pupae and adults

The results from the larval assays suggest that deviation from optimal temperatures imposes a lethal cost, with concomitant reduction in pupation and emergence net growth. The predicted optimal temperature for larval survival was ~24.60°C, with the lowest mortalities recorded at 25-28°C, and within 24-72 h period post exposure, and extreme cold and heat increasing mortality linearly. Several studies have documented similar patterns. For example, (Rocca *et al.*, 2009) using laboratory domesticated colonies have reported that 40°C heat stress for 1.5-2 h led to about 50% mortalities in *An. gambiae* larvae. However, the above studies utilized not only a population from a different locality, but also the mortalities were recorded only at 24 h, not aggregated up till 192 h period. It is also possible that using circulating water bath in this study leads to a more even temperature distribution and precision, capturing thermal susceptibility phenotype better than a water bath. Although using controlled rearing of lab A*nopheles gambiae* s.s. under a temperature regimen (Christiansen-Jucht *et al.*, 2014) reported that increasing temperature during larval stages significantly increased larval mortality; importantly, all larvae reared at 35°C died before adult emergence. In other species, like *Ae. aegypti,* short and acute larval exposure at high temperatures increased mortalities linearly, 90% mortality at 44°C and absolute mortality at 46°C (Sivan *et al.*,

679 2021). The temperature, 42°C, was found to be diagnostic for mortality in *Culex pipiens pallens*
680 (Padde *et al.*, 2024).When larvae were exposed for three days at various temperatures, the authors
681 suggested 33°C as the adaptable temperature, 37°C as the critical temperature, and 42°C as fatal.
682 Several studies have established the carryover impact of larval thermal stress on pupation and
683 emergence, as well as on other phenotypes, including adult size and longevity, not characterized
684 in this study. For example, under constant temperature exposure (Bayoh and Lindsay, 2003) have
685 established that *An. gambiae* development rate increased with temperature to a peak around 28°C,
686 and then declined. Adult development rate was greatest around 28–32°C, but emergence was
687 highest around 22–26°C, and no adults emerged below 18°C or above 34°C. This is in agreement
688 with some of our findings, of maximal pupation and emergence of ~85% around 25°C, and with
689 temperatures between 22-25°C predicted as the optimal range for pupation and emergence, while
690 extremes below 15°C and above 37°C reduce net growth. The finding that all *An. gambiae s.s.*
691 larvae reared continuously at 35°C died before adult emergence (Christiansen-Jucht *et al.*, 2014)
692 strongly suggests that temperatures above 35°C are critically non-permissible for natural growth
693 of *Anopheles*. The wide gap in pupation between 20°C and 35°C, observed in this study could be
694 due to preheating at the larval stage, which usually leads to hardening, increasing thermal tolerance
695 in subsequent stages (Bayoh and Lindsay, 2003; Rocca *et al.*, 2009). In *Culex pipiens pallens*, high,
696 constant temperatures for 3 d significantly decreased larval development time, growth rate and
697 adult emergence (Padde *et al.*, 2024), with sublethal carry-over effects (larvae that survived 37°C
698 exposure produced adults with impaired reproductive output).
699
700

4.3 Temperature extremes reduce pupal survival and impose carry-over effect on its adult emergence

Stage-specific thermal stress imposed significance fitness cost on *An. coluzzii* pupae, inflicting mortalities and reducing adult emergence significantly. The lowest pupal mortality rate (3%) for the control pupae was 5 times lower than the 15% mortalities observed in control larvae; and the differences in mortalities at 42°C (mortality of 40% in pupae and 52% in larvae) suggests higher thermal resilience in the pupae. Indeed, pupae were known to be generally more resistant than larvae to thermal stress at 40°C (Rocca *et al.*, 2009). Another study which employed acute thermal exposure for 2 h spanning extremely cold and extremely high temperatures (Lyons *et al.*, 2012), has established that larvae and pupae of both *An. arabiensis* and *An. funestus* as having comparable upper lethal temperatures, while the pupae demonstrate more tolerance to lower lethal temperatures. The greater thermal tolerance observed in pupae compared with larvae may reflect stage-specific differences in cuticular sclerotization and mechanical resistance, as sclerotization hardens and stabilizes the insect cuticle (Hopkins and Kramer, 1992; Hopkins *et al.*, 2000), whereas newly formed cuticle during molting in actively developing larvae may make them more vulnerable. The above evidences support the use of pupal-specific thermal exposure followed by adult emergence as a robust endpoint for assessing carry-over effects of acute temperature stress.

4.4 2La chromosomal inversion is associated with larval thermal tolerance

Direct experimental evidence linking the $2L^a$ inversion to thermal tolerance in field sourced *Anopheles* remains limited, with the strongest support coming from larval heat-stress assays using lab colonies and field-derived *An. gambiae* s.l. populations. Our findings confirmed once more the role of this inversion polymorphism in thermal tolerance in *An. coluzzii* larvae. The finding of association between larval heat tolerance and $2L^a$ homozygote inversion genotypes was similar to

our previous observation on *An. coluzzii* larvae from Kano, Nigeria (Ibrahim *et al.*, 2021). Several studies have previously established the role of this inversion in thermal tolerance in *Anopheles* mosquitoes. For example, (Rocca *et al.*, 2009) showed that heat-hardened *An. gambiae* larvae bearing the $2L^{a}$ inversion genotype survived significantly better than their $2L^{a+}$ counterparts. Thermal tolerance in insects has a genetic basis, as shown by divergent heat-stress transcriptional responses between alternative $2L^{a}$ arrangements in *Anopheles gambiae* larvae (Cassone *et al.*, 2011), family-level variation and heat-shock gene expression differences in *Ae. aegypti* (Ware-Gilmore *et al.*, 2023), and chromosomal inversion-associated variation in heat and cold resistance in *D. melanogaster* (Rako *et al.*, 2007).

4.5 1014F *kdr* mutation is associated with larval thermal tolerance

In addition to insecticide resistance, previous studies have shown several phenotypes associated with the 1014F *kdr* mutation. For example, male mating competitiveness with the L1014/1014F heterozygote genotype (Platt et al. 2015); blood feeding success rates in insecticide-resistant *Anopheles* mosquitoes (Diop et al. 2021); and reduced vector competence in a microbiota-dependent manner in *An. coluzzii* (Nardini *et al.*, 2023). However, prior to this study little is known about the role of this mutation in temperature sensitivity, although (Kristan, Abeku and Lines, 2018) have examined how environmental temperature, humidity, insecticide exposure and *kdr* genotype influenced survival of wild *Anopheles gambiae* s.s. But this study did not directly demonstrate that the 1014F *kdr* mutation is directly associated with heat tolerance.

The *vgsc* is essential for neuronal excitability because it initiates and propagate action potentials in excitable cells, making this locus a plausible candidate for traits involving temperature-sensitive

neuromuscular performance (Dong *et al.*, 2014). Channel gating is intrinsically temperature-dependent, and biophysical modelling shows that temperature alters the activation kinetics of sodium, potassium and calcium conductance, thereby influencing action-potential generation, firing frequency and neuronal stability under thermal stress (Miller *et al.*, 2025). We found this mutation to be associated with heat tolerance, but only in heterozygote state. The high proportion of heterozygote genotype among the heat-tolerant larvae, coupled with the high proportion of homozygote resistant genotype among the more heat-sensitive larvae suggests that heat tolerance is associated with heterozygosity, while homozygosity possibly imposes undesirable fitness cost.

In *D. melanogaster*, mutations affecting *vgsc* have been associated with reversible temperature-induced paralysis, demonstrating that altered sodium-channel function can disrupt neuromuscular activity under thermal stress (Jackson *et al.*, 1984). Similarly, dominant cold-sensitive out-cold mutants were mapped to novel missense mutations in the *vgsc* paralytic (para), linking *vgsc* variation specifically to cold-induced paralysis phenotypes (Lindsay *et al.*, 2008). In addition, reduced sodium-channel abundance in mlenapts homozygous mutant flies caused both cold- and heat-sensitive developmental lethality, indicating that sodium-channel function can influence survival and development across thermal extremes (Garber *et al.*, 2012).

5. Conclusions

This study established that acute temperature significantly constrain the survival of the immature stages of the major malaria vector, *An. coluzzii*, negatively affecting key fitness traits, including egg hatching, larval pupation, and pupal emergence to adults. Thermal performance curve predicted the optimal temperatures for the above life processes to be between 22-28°C, with temperatures below and above these ranges reducing fitness. In general, pupae were found to have

higher thermal breadth compared to larvae and eggs, with eggs being the most sensitive life stage. For larvae and pupae, the temperature, 42°C, was clearly the critical thermal maxima beyond which survival and development cease.

Stage-structured modelling reveals that temperature affects not only the absolute abundance of each immature stage but also the flow of individuals towards the adult stage, the only stage that transmits *Plasmodium*, which was reduced by more than one third. The modelling highlights the link between the experimental thermal tolerance data presented in this paper and the predicted impact of climate warming on *An. coluzzii* population dynamics and malaria transmission risk.

Genotyping results indicate that the $2L^a$ chromosomal inversion polymorphism and the L1014F *kdr* mutation are associated with larval heat tolerance, suggesting that these pleiotropic genomic changes may confer thermal tolerance in this malaria mosquito.

These findings provide an insight into the temperature dependence of survival and development of immature stages, and a glimpse at the mechanism mosquitoes will likely employ to adjust to future temperature extremes, with relevance to understanding population dynamics of this malaria mosquito, and its malaria transmission risk in the future warmer world.

List of Abbreviations

% = percent

~ = approximately

°C = degrees Celsius

µL = microlitre

Ae. = Aedes

An. = Anopheles

bp = base pair

CI = confidence interval

CTIDR = Centrum for Tropical and Infectious Diseases Research

d = day

D. = Drosophila

ddH20 = double distilled water

df = degree of freedom

F0 = parental generation

F1 = first filial generation

gDNA = genomic deoxyribonucleic acids

h = hour

kdr = knockdown resistance

LT50 = lethal temperature 50

min = minutes

mL = millilitre

mM = millimolar

PCR = polymerase chain reaction

s = seconds

s.s. = sensu stricto

vgsc = voltage gated sodium channel

$\chi 2$ = Chi square

Declarations

Ethics approval and consent to participate

Clearance for field work and ethical approval was granted by Jigawa State Federal Ministry of Health (Authorization Number JGHREC/2024/0054, dated 12/03/2024). Prior to collection, a meeting was held with the local chief and the village people to explain the aim of the study and its benefits. No written and/or signed informed consent was obtained as no collection of indoor resting, blood fed mosquitoes was conducted.

Consent for publication

Not applicable

Availability of Data

Data generated or analysed during this study are included in this published article (and its supplementary information files).

Competing interests

The authors declare that they have no competing interests.

Funding

This study was funded by the Wellcome Trust Career Development Award grant (# 225937/Z/22/Z) to SSI. The funder has no role in the conceptualization, design, data collection, analysis, decision to publish, or preparation of this manuscript.

Authors' contribution

Conceived and designed by SSI. HAA, UAm, AAZ, YYA, SA and AHS conducted the laboratory phenotyping of mosquitoes. HAA, HKE, MMM, and KA conducted molecular analyses. SSS, HAA, UAb, IWZ, MAS, and IAB conducted data analyses. SSI wrote the manuscript with contribution from HAA, MAS, IAB, UCN and CSW. All authors read and approved the final manuscript.

Acknowledgments

Not Applicable.

References

Anee, H.K. *et al.* (2021) 'Effect of temperature on life cycle and behaviour of Aedes aegypti (Diptera: Culicidae)', *Bangladesh Journal of Zoology*, 49(3), pp. 369–379.

Arifin, S.M.N. *et al.* (2014) 'An agent-based model of the population dynamics of Anopheles gambiae', *Malaria Journal*, 13, p. 424. Available at: https://doi.org/10.1186/1475-2875-13-424.

Ayala, D., Ullastres, A. and González, J. (2014) 'Adaptation through chromosomal inversions in Anopheles', *Frontiers in Genetics*, 5, p. 129. Available at: https://doi.org/10.3389/fgene.2014.00129.

Bayoh, M.N. and Lindsay, S.W. (2003) 'Effect of temperature on the development of the aquatic stages of Anopheles gambiae sensu stricto (Diptera: Culicidae)', *Bulletin of Entomological Research*, 93(5), pp. 375–381. Available at: https://doi.org/10.1079/ber2003259.

Beck-Johnson, L.M. *et al.* (2013) 'The effect of temperature on Anopheles mosquito population dynamics and the potential for malaria transmission', *PloS One*, 8(11), p. e79276. Available at: https://doi.org/10.1371/journal.pone.0079276.

Brooke, B.D., Hunt, R.H. and Coetzee, M. (2000) 'Resistance to dieldrin + fipronil assorts with chromosome inversion 2La in the malaria vector Anopheles gambiae', *Medical and Veterinary Entomology*, 14(2), pp. 190–194. Available at: https://doi.org/10.1046/j.1365-2915.2000.00222.x.

867 Cassone, B.J. *et al.* (2011) 'Divergent transcriptional response to thermal stress by Anopheles
868 gambiae larvae carrying alternative arrangements of inversion 2La', *Molecular Ecology*, 20(12),
869 pp. 2567–2580. Available at: https://doi.org/10.1111/j.1365-294X.2011.05114.x.

870 Christiansen-Jucht, C. *et al.* (2014) 'Temperature during larval development and adult
871 maintenance influences the survival of Anopheles gambiae s.s.', *Parasites & Vectors*, 7(1), p.
872 489. Available at: https://doi.org/10.1186/s13071-014-0489-3.

873 Christiansen-Jucht, C.D. *et al.* (2015) 'Larval and adult environmental temperatures influence
874 the adult reproductive traits of Anopheles gambiae s.s.', *Parasites & Vectors*, 8(1), p. 456.
875 Available at: https://doi.org/10.1186/s13071-015-1053-5.

876 Coetzee, M. (2020) 'Key to the females of Afrotropical Anopheles mosquitoes (Diptera:
877 Culicidae)', *Malaria Journal*, 19(1), p. 70. Available at: https://doi.org/10.1186/s12936-020-
878 3144-9.

879 Colinet, H. *et al.* (2015) 'Insects in fluctuating thermal environments', *Annual Review of*
880 *Entomology*, 60, pp. 123–140. Available at: https://doi.org/10.1146/annurev-ento-010814-
881 021017.

882 Coluzzi, M. *et al.* (1979) 'Chromosomal differentiation and adaptation to human environments
883 in the Anopheles gambiae complex', *Transactions of the Royal Society of Tropical Medicine and*
884 *Hygiene*, 73(5), pp. 483–497. Available at: https://doi.org/10.1016/0035-9203(79)90036-1.

885 Couper, L.I. *et al.* (2021) 'How will mosquitoes adapt to climate warming?', *eLife*, 10, p. e69630.
886 Available at: https://doi.org/10.7554/eLife.69630.

887 Couper, L.I. *et al.* (2024) 'Mosquito thermal tolerance is remarkably constrained across a large
888 climatic range', *Proceedings. Biological Sciences*, 291(2015), p. 20232457. Available at:
889 https://doi.org/10.1098/rspb.2023.2457.

890 Dong, K. *et al.* (2014) 'Molecular biology of insect sodium channels and pyrethroid resistance',
891 *Insect Biochemistry and Molecular Biology*, 50, pp. 1–17. Available at:
892 https://doi.org/10.1016/j.ibmb.2014.03.012.

893 Fouet, C. *et al.* (2012) 'Adaptation to aridity in the malaria mosquito Anopheles gambiae:
894 chromosomal inversion polymorphism and body size influence resistance to desiccation', *PloS*
895 *One*, 7(4), p. e34841. Available at: https://doi.org/10.1371/journal.pone.0034841.

896 Garber, G. *et al.* (2012) 'Effect of sodium channel abundance on Drosophila development,
897 reproductive capacity and aging', *Fly*, 6(1), pp. 57–67. Available at:
898 https://doi.org/10.4161/fly.18570.

899 Gray, E.M. *et al.* (2009) 'Inversion 2La is associated with enhanced desiccation resistance in
900 Anopheles gambiae', *Malaria Journal*, 8, p. 215. Available at: https://doi.org/10.1186/1475-
901 2875-8-215.

Hoegh-Guldberg, O. *et al.* (2018) 'Impacts of 1.5°C Global Warming on Natural and Human Systems', in V. Masson-Delmotte et al. (eds) *Global warming of 1.5°C.* IPCC Secretariat, pp. 175–311. Available at: https://www.ipcc.ch/sr15/chapter/chapter-3/ (Accessed: 18 January 2026).

Hopkins, T.L. *et al.* (2000) 'Pupal cuticle proteins of Manduca sexta: characterization and profiles during sclerotization', *Insect Biochemistry and Molecular Biology*, 30(1), pp. 19–27. Available at: https://doi.org/10.1016/s0965-1748(99)00091-0.

Hopkins, T.L. and Kramer, K.J. (1992) 'Insect Cuticle Sclerotization', *Annual Review of Entomology*, 37(1), pp. 273–302. Available at: https://doi.org/10.1146/annurev.en.37.010192.001421.

Huang, J. *et al.* (2006) 'Daily temperature profiles in and around Western Kenyan larval habitats of Anopheles gambiae as related to egg mortality', *Malaria Journal*, 5, p. 87. Available at: https://doi.org/10.1186/1475-2875-5-87.

Ibrahim, S.S. *et al.* (2014) 'High frequency of kdr L1014F is associated with pyrethroid resistance in Anopheles coluzzii in Sudan savannah of northern Nigeria', *BMC infectious diseases*, 14, p. 441. Available at: https://doi.org/10.1186/1471-2334-14-441.

Ibrahim, S.S. *et al.* (2021) '2La Paracentric Chromosomal Inversion and Overexpressed Metabolic Genes Enhance Thermotolerance and Pyrethroid Resistance in the Major Malaria Vector Anopheles gambiae', *Biology*, 10(6), p. 518. Available at: https://doi.org/10.3390/biology10060518.

Impoinvil, D.E. *et al.* (2007) 'Constant temperature and time period effects on Anopheles gambiae egg hatching', *Journal of the American Mosquito Control Association*, 23(2), p. 124.

IPCC (2022) *Global Warming of 1.5°C: IPCC Special Report on Impacts of Global Warming of 1.5°C above Pre-industrial Levels in Context of Strengthening Response to Climate Change, Sustainable Development, and Efforts to Eradicate Poverty*. 1st edn. Cambridge University Press. Available at: https://doi.org/10.1017/9781009157940.

Jackson, F.R. *et al.* (1984) 'Two types of mutants affecting voltage-sensitive sodium channels in Drosophila melanogaster', *Nature*, 308(5955), pp. 189–191. Available at: https://doi.org/10.1038/308189a0.

Kale, G. *et al.* (2023) 'Elevated temperature fatally disrupts nuclear divisions in the early Drosophila embryo', *bioRxiv*, pp. 2023–09.

Kramer, I.M. *et al.* (2026) 'Heatwaves Constrain the Future Persistence of Mosquito Vectors in Europe', *Global Change Biology*, 32(4), p. e70876. Available at: https://doi.org/10.1111/gcb.70876.

Kristan, M., Abeku, T.A. and Lines, J. (2018) 'Effect of environmental variables and kdr resistance genotype on survival probability and infection rates in Anopheles gambiae (s.s.)', *Parasites & Vectors*, 11(1), p. 560. Available at: https://doi.org/10.1186/s13071-018-3150-8.

Lindsay, H.A. *et al.* (2008) 'The dominant cold-sensitive Out-cold mutants of Drosophila melanogaster have novel missense mutations in the voltage-gated sodium channel gene paralytic', *Genetics*, 180(2), pp. 873–884. Available at: https://doi.org/10.1534/genetics.108.090951.

Livak, K.J. (1984) 'Organization and mapping of a sequence on the Drosophila melanogaster X and Y chromosomes that is transcribed during spermatogenesis', *Genetics*, 107(4), pp. 611–634. Available at: https://doi.org/10.1093/genetics/107.4.611.

Lyons, C.L. *et al.* (2012) 'Thermal limits of wild and laboratory strains of two African malaria vector species, Anopheles arabiensis and Anopheles funestus', *Malaria Journal*, 11, p. 226. Available at: https://doi.org/10.1186/1475-2875-11-226.

Martinez-Torres, D. *et al.* (1998) 'Molecular characterization of pyrethroid knockdown resistance (kdr) in the major malaria vector Anopheles gambiae s.s', *Insect Molecular Biology*, 7(2), pp. 179–184. Available at: https://doi.org/10.1046/j.1365-2583.1998.72062.x.

Miller, J.A. *et al.* (2025) 'Incorporating the thermodynamic effects of temperature and pressure on modeling neuronal gating kinetics', *PloS One*, 20(10), p. e0333592. Available at: https://doi.org/10.1371/journal.pone.0333592.

Mordecai, E.A. *et al.* (2013) 'Optimal temperature for malaria transmission is dramatically lower than previously predicted', *Ecology Letters*, 16(1), pp. 22–30. Available at: https://doi.org/10.1111/ele.12015.

Mordecai, E.A. *et al.* (2019) 'Thermal biology of mosquito-borne disease', *Ecology Letters*, 22(10), pp. 1690–1708. Available at: https://doi.org/10.1111/ele.13335.

Nardini, L. *et al.* (2023) 'The voltage-gated sodium channel, para, limits Anopheles coluzzii vector competence in a microbiota dependent manner', *Scientific Reports*, 13(1), p. 14572. Available at: https://doi.org/10.1038/s41598-023-40432-x.

Nguyen, V.T., Morange, M. and Bensaude, O. (1989) 'Protein denaturation during heat shock and related stress. Escherichia coli beta-galactosidase and Photinus pyralis luciferase inactivation in mouse cells', *The Journal of Biological Chemistry*, 264(18), pp. 10487–10492.

Oliver, S.V. and Brooke, B.D. (2017) 'The effect of elevated temperatures on the life history and insecticide resistance phenotype of the major malaria vector Anopheles arabiensis (Diptera: Culicidae)', *Malaria Journal*, 16(1), p. 73. Available at: https://doi.org/10.1186/s12936-017-1720-4.

Paaijmans, K.P. *et al.* (2010) 'Influence of climate on malaria transmission depends on daily temperature variation', *Proceedings of the National Academy of Sciences*, 107(34), pp. 15135–15139. Available at: https://doi.org/10.1073/pnas.1006422107.

Padde, J.R. *et al.* (2024) 'Adaptation and carry over effects of extreme sporadic heat stress in Culex mosquitoes', *Acta Tropica*, 260, p. 107417.

Pazmiño-Betancourth, M. *et al.* (2026) 'Stage-dependent trade-offs in thermal performance: fluctuating temperatures reverse larval and adult fitness in Anopheles gambiae and An. coluzzii', *Journal of Medical Entomology*, 63(1), p. tjaf189. Available at: https://doi.org/10.1093/jme/tjaf189.

Petros, L.D. *et al.* (2025) 'Age-structured malaria model with temperature-dependent dynamics and optimal control analysis within a partial differential equation framework', *PloS One*, 20(8), p. e0330158. Available at: https://doi.org/10.1371/journal.pone.0330158.

Pu, J., Wang, Z. and Chung, H. (2020) 'Climate change and the genetics of insecticide resistance', *Pest Management Science*, 76(3), pp. 846–852. Available at: https://doi.org/10.1002/ps.5700.

Rako, L. *et al.* (2007) 'Candidate genes and thermal phenotypes: identifying ecologically important genetic variation for thermotolerance in the Australian Drosophila melanogaster cline', *Molecular Ecology*, 16(14), pp. 2948–2957. Available at: https://doi.org/10.1111/j.1365-294X.2007.03332.x.

Ranasinghe et al., (2023) *Climate Change Information for Regional Impact and for Risk Assessment. In Climate Change 2021 – The Physical Science Basis: Contribution of Working Group I to the Sixth Assessment Report of the Intergovernmental Panel on Climate Change*. 1st edn. Cambridge University Press. Available at: https://doi.org/10.1017/9781009157896.

Ren, Z. *et al.* (2016) 'Predicting malaria vector distribution under climate change scenarios in China: Challenges for malaria elimination', *Scientific Reports*, 6, p. 20604. Available at: https://doi.org/10.1038/srep20604.

Riehle, M.M. *et al.* (2017) 'The Anopheles gambiae 2La chromosome inversion is associated with susceptibility to Plasmodium falciparum in Africa', *eLife*, 6, p. e25813. Available at: https://doi.org/10.7554/eLife.25813.

Rocca, K.A.C. *et al.* (2009) '2La chromosomal inversion enhances thermal tolerance of Anopheles gambiae larvae', *Malaria Journal*, 8, p. 147. Available at: https://doi.org/10.1186/1475-2875-8-147.

Roux, O. *et al.* (2015) 'Evidence for carry-over effects of predator exposure on pathogen transmission potential', *Proceedings. Biological Sciences*, 282(1821), p. 20152430. Available at: https://doi.org/10.1098/rspb.2015.2430.

Ryan, S.J., Lippi, C.A. and Zermoglio, F. (2020) 'Shifting transmission risk for malaria in Africa with climate change: a framework for planning and intervention', *Malaria Journal*, 19(1), p. 170. Available at: https://doi.org/10.1186/s12936-020-03224-6.

Santolamazza, F. *et al.* (2008) 'Insertion polymorphisms of SINE200 retrotransposons within speciation islands of Anopheles gambiae molecular forms', *Malaria Journal*, 7, p. 163. Available at: https://doi.org/10.1186/1475-2875-7-163.

Sivan, A. *et al.* (2021) 'Thermotolerance and acclimation in the immature stages of Aedes aegypti (L) (Diptera: Culicidae) to simulated thermal stress', *International Journal of Tropical Insect Science*, 41(1), pp. 333–344. Available at: https://doi.org/10.1007/s42690-020-00211-x.

Sukiato, F. *et al.* (2019) 'The effects of temperature and shading on mortality and development rates of Aedes aegypti (Diptera: Culicidae)', *Journal of Vector Ecology*, 44(2), pp. 264–270. Available at: https://doi.org/10.1111/jvec.12358.

Traoré, B. *et al.* (2021) 'A temperature-dependent mathematical model of malaria transmission with stage-structured mosquito population dynamics', *Nonautonomous Dynamical Systems*, 8(1), pp. 267–296. Available at: https://doi.org/10.1515/msds-2020-0138.

Villena, O.C. *et al.* (2022) 'Temperature impacts the environmental suitability for malaria transmission by *Anopheles gambiae* and *Anopheles stephensi*', *Ecology*, 103(8), p. e3685. Available at: https://doi.org/10.1002/ecy.3685.

Ware-Gilmore, F. *et al.* (2023) 'Assessing the role of family level variation and heat shock gene expression in the thermal stress response of the mosquito Aedes aegypti', *Philosophical Transactions of the Royal Society of London. Series B, Biological Sciences*, 378(1873), p. 20220011. Available at: https://doi.org/10.1098/rstb.2022.0011.

White, B.J. *et al.* (2007) 'Molecular karyotyping of the 2La inversion in Anopheles gambiae', *The American Journal of Tropical Medicine and Hygiene*, 76(2), pp. 334–339.

WHO (2023) *Climate change and health [Fact sheet].* World Health Organization. Available at: https://www.who.int/news-room/fact-sheets/detail/climate-change-and-health (Accessed: 19 February 2026).

WHO, W.H.O. (2025) *World malaria report 2025: Addressing the threat of antimalarial drug resistance*. World Health Organization.

Wondji, C. *et al.* (2005) 'Species and populations of the Anopheles gambiae complex in Cameroon with special emphasis on chromosomal and molecular forms of Anopheles gambiae s.s', *Journal of Medical Entomology*, 42(6), pp. 998–1005. Available at: https://doi.org/10.1093/jmedent/42.6.998.

Figure Legends

Figure 1: Impact of temperature on egg hatching in *An. coluzzii.* a. thermal performance curve showing relationship between egg hatching rates and experimental temperatures; **b**. a line graph predicting the impact of temperature on net population change; **c.** a heatmap showing the mean percentage of eggs that successfully hatched at each temperature–time combination, identifying the temperature range and time point associated with maximum hatching success.

Figure 2: Impact of temperature on larval survival and development rate. a. thermal performance curve showing relationship between larval mortality and temperatures; **b.** heatmap displaying the percentage of dead larvae at each time-temperature combination; **c.** thermal performance curve showing the carryover effect of temperature on larval pupation; **d.** a heatmap showing the percentage of larvae that successfully advanced to the pupal stage with time.

Figure 3: Stage-specific impact of temperature on pupal survival and development rate. a. thermal performance curve showing relationship between pupal mortality and temperatures; **b.** a heatmap displaying percentage pupal mortality at each time-temperature combinations; **c.** thermal performance curve showing relationship between adult emergence and stage-specific temperature treatments; **d.** a heatmap displaying percentage pupal emergence to adults at each time-temperature combinations.

Figure 4: Multiple correspondence analysis showing relationship between heat tolerance and 2L^{a} inversion genotypes. a. asymmetric/biplot featuring larval variables on dimensions 1 and 2. Variable categories with similar profiles are grouped together. Negatively correlated variable categories are positioned on the opposite side of the plot origin (opposed quadrants). Variables cluster close to the pole, positive or negative of each dimension indicating how important is their contribution to the dimension; **b.** cos2 plot showing the inertia contribution of the various larval variables; **c.** biplot featuring pupal variables on dimensions 1 and 2; **d.** cos2 plot showing inertia contribution of the various pupal variables.

Figure 5: Multiple correspondence analysis showing relationship between heat tolerance and the 1014F *kdr* mutation genotypes. **a.** a biplot featuring larval variables on dimensions 1 and 2. Variable categories with similar profiles are grouped together. Negatively correlated variable categories are positioned on the opposite side of the plot origin (opposed quadrants). Variables cluster close to the pole, positive or negative of each dimension indicating how important is their

contribution to the dimension; **b.** cos2 plot showing the inertia contribution of the various larval variables, with SS contributing the most inertia.

Supplementary Figures Legends

Figure S1: Agarose gel showing 479bp bands characteristic of *An. coluzzii* species. Lanes 1 and 22 are hyperladder 50bp, 50-1013bp (GDSBio, Guangzhou, China). Lanes 2, 3 and 4 are *An. coluzzii*, *An. gambiae s.s.*, and *An. arabiensis* positive control samples. Lane 5 is negative control, with ddH_20. Samples 1–16 (lanes 6–21) are *An. coluzzii*.

Figure S2: Kaplan-Meier survivorship analysis of the larvae exposed to various temperature treatments.

Figure S3: Carryover impact of temperature on larval survival and development. a. Comparison of pupation success rate and larval mortality rate as functions of temperature; **b.** Failure/success ratio (mortality rate divided by pupation rate) of larvae. Ratios below 1 indicate more successes than failures; **c.** thermal performance curve of the impact of carryover temperatures on adult emergence from heated larvae.

Figure S4: Kaplan-Meier survivorship analysis of the pupae exposed to various temperatures.

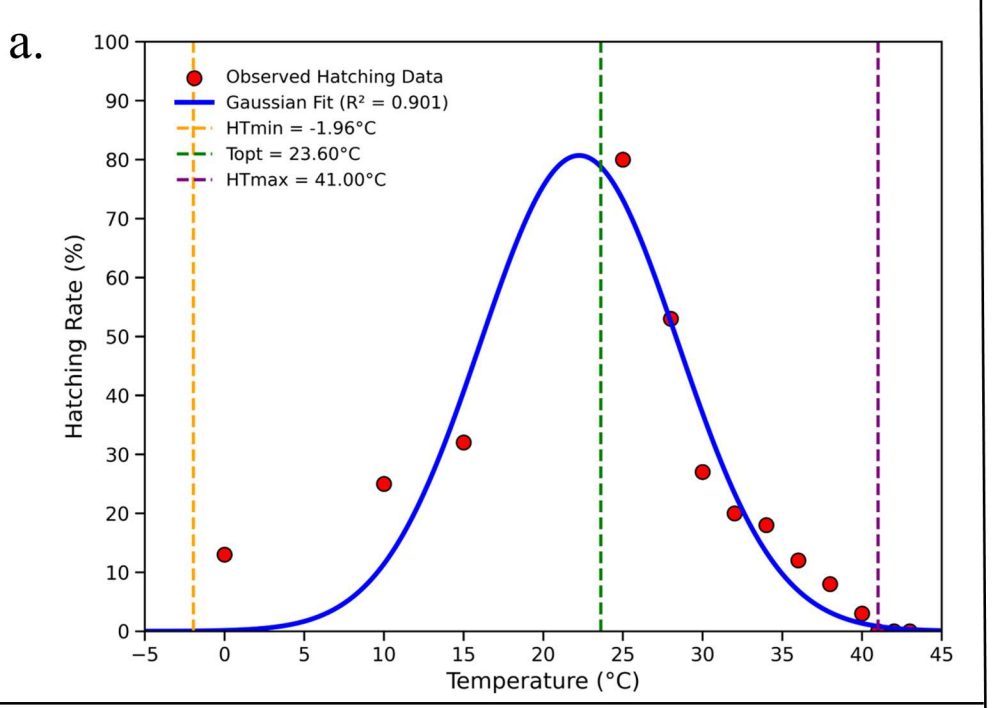
Figure S5: Dynamics of pupal mortality and emergence from stage-specific temperature exposures. a. Failure/success ratio (mortality rate divided by pupal emergence rate) of larvae. Ratios below 1 indicate more successes than failures; **b.** line graph showing predicted net population change of pupae (successful adult emergence minus pupal mortality) across a temperature range of 0–43°C. Positive net change indicates net adult emergence, while negative net change indicates net pupal death.

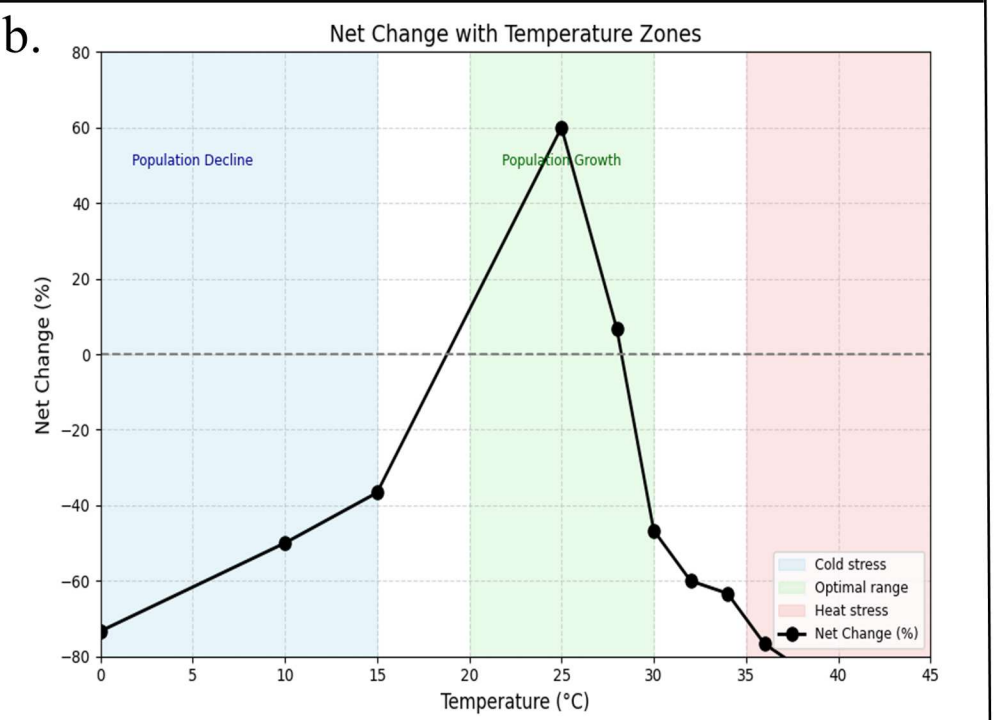
Figure S6: Agarose gel illustrating the $2L^a$ genotypes of *An. coluzzii* larvae exposed to heat. **a.** larvae alive at 41°C, samples 1-25; **b.** larvae alive at 41°C samples 26-50 **c**. larvae dead at 38°C samples 1-25; **d.** larvae dead at 38°C samples 26-50. In each upper panel lane 1 and last lanes are the hyperladder 100bp (Bioline, London, UK), and lanes 2, 3 and 4 panels are positive controls for $2L^a/2L^a$ homozygote inverted karyotype, $2L^{+a}/2L^{+a}$ homozygote standard arrangement and $2L^a/2L^{+a}$ heterozygote arrangement, respectively.

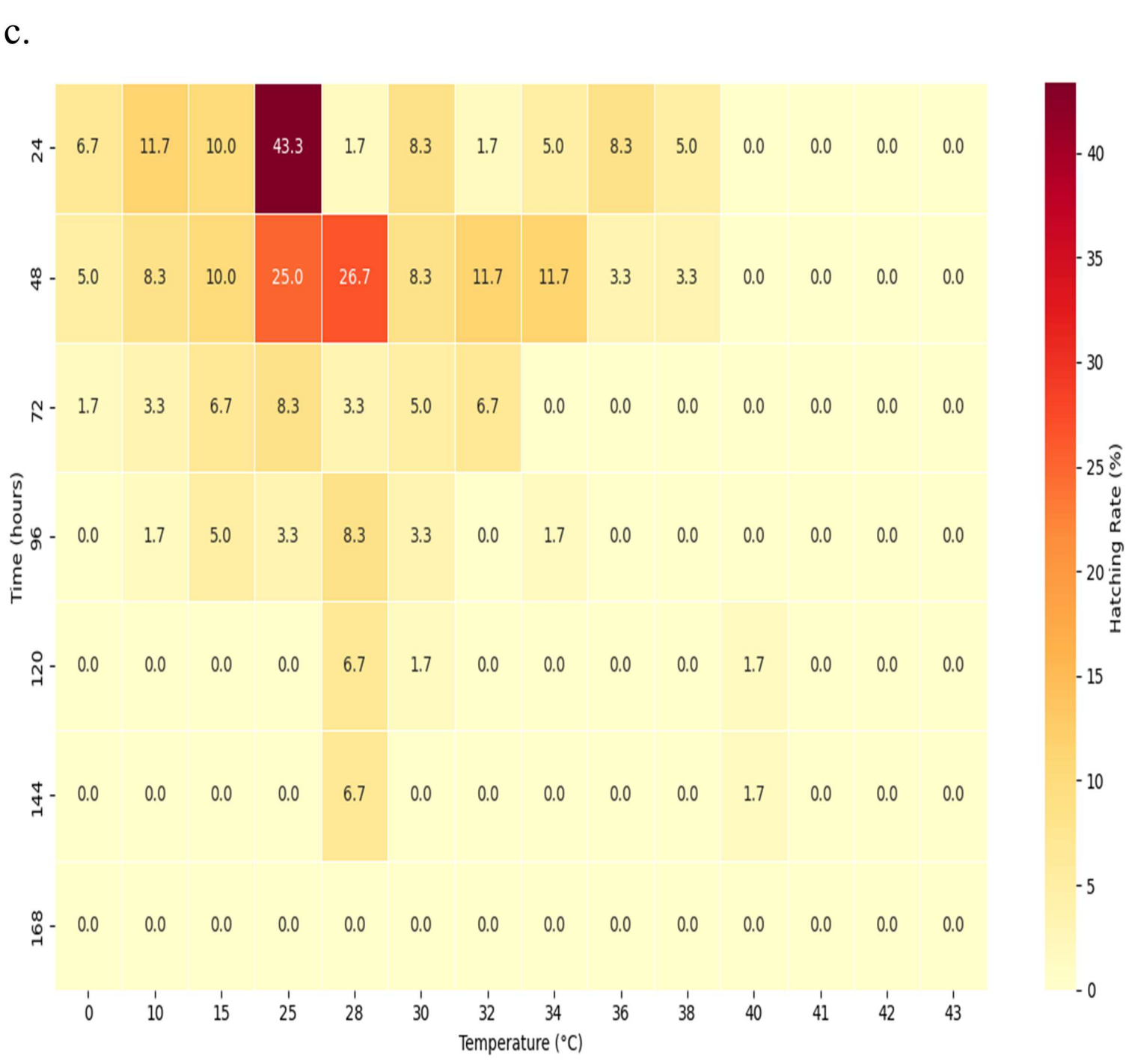
Figure S7: Agarose gel illustrating the $2L^a$ genotypes of *An. coluzzii* pupae exposed to heat. **a.** pupae alive at 41°C; and **b.** pupae dead at 38°C. In each upper panel lane 1 and the last lanes are the hyperladder 100bp (Bioline, London, UK), and lanes 2, 3 and 4are positive controls for $2L^a/2L^a$ homozygote inverted arrangement, $2L^{+a}/2L^{+a}$ homozygote standard arrangement and $2L^a/2L^{+a}$ heterozygote arrangement, respectively.

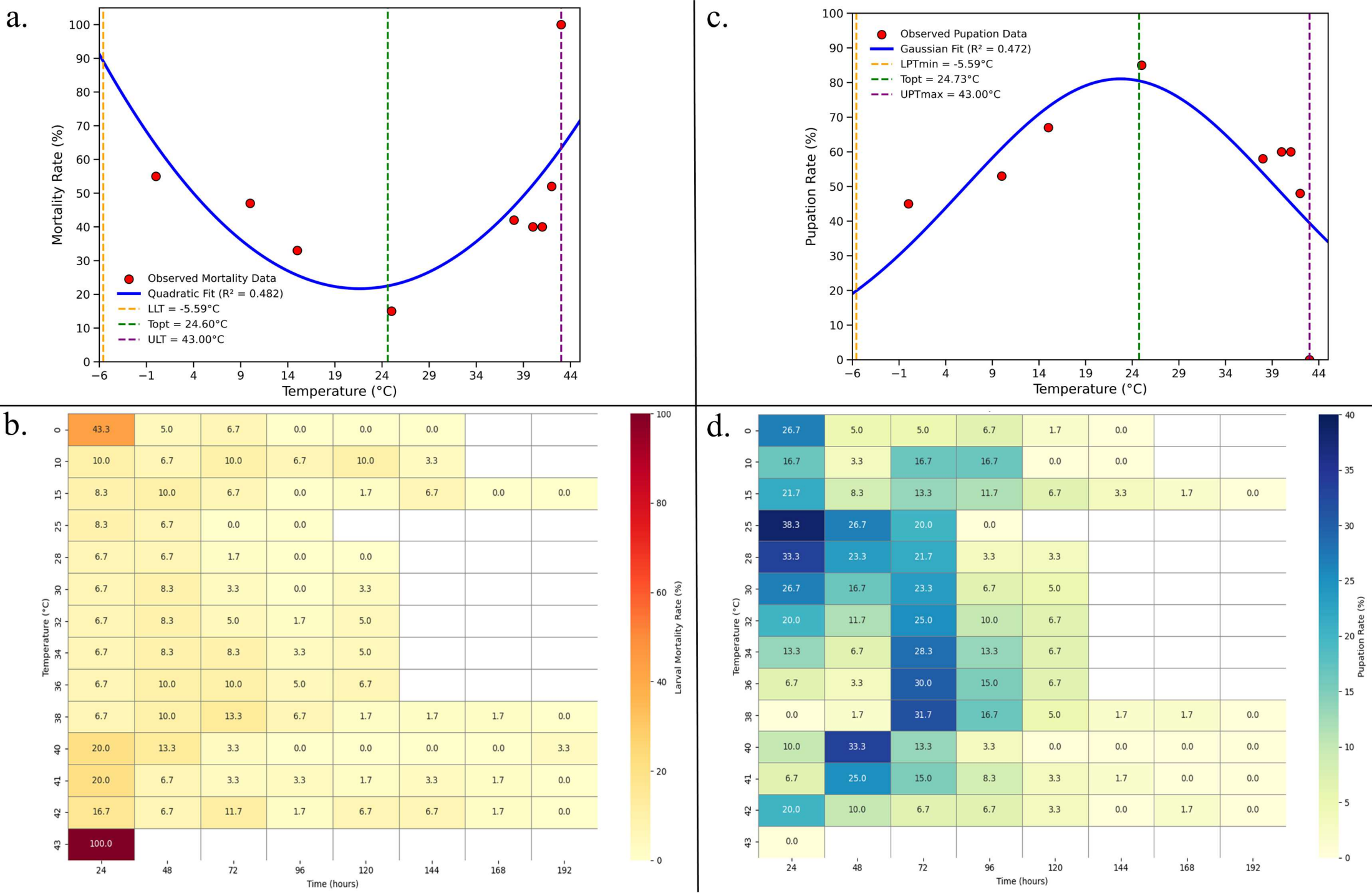
Figure S8: Relative contribution of variables on the MCA factor map. a. Scree plot of three dimensions explaining contribution of the respective feature inputs from $2L^a$ larval phenotype vs genotype data; **b**. Scree plot of three dimensions explaining contribution of the respective feature inputs from $2L^a$ pupal genotype vs phenotype data; **c.** Scree plot of three dimensions explaining contribution of the respective feature inputs from 1014F *kdr* larval genotype vs phenotype data.

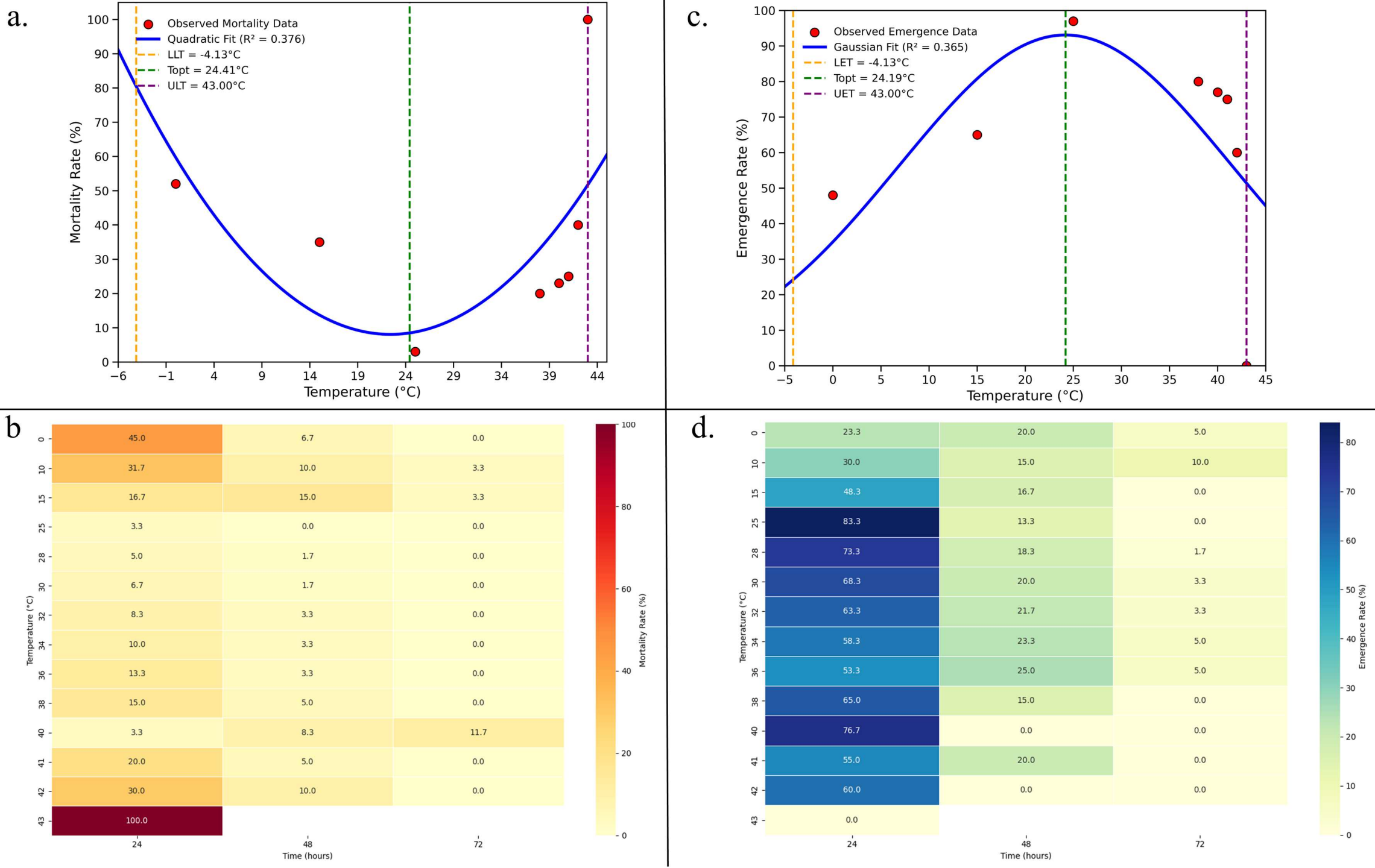
Figure S9: Agarose gel illustrating the L1014F *kdr* genotypes of *An. coluzzii* larvae exposed to heat. a. larvae alive at 41°C, samples 1-25; **b.** larvae alive at 41°C samples 26-50 **c**. larvae dead at 38°C samples 1-25; **d.** larvae dead at 38°C samples 26-50. In each upper panel lane 1 is the hyperladder 100bp (Bioline, London, UK), and lanes 2, 3 and 4 in all upper panels are positive controls for homozygote resistant (1014F/1014F), homozygote susceptible (L1014/L1014) and heterozygote (L1014/1014F) kdr genotypes, respectively.

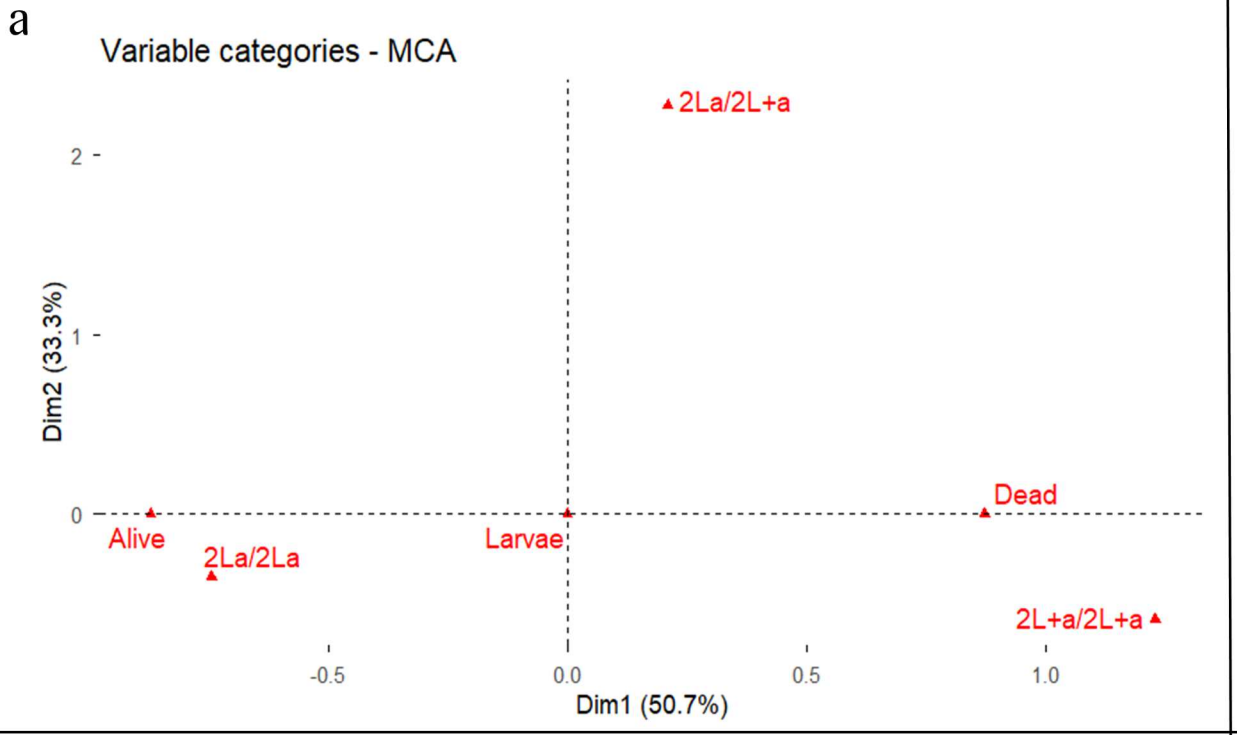

a.
Observed Hatching Data
Gaussian Fit (R² = 0.901)
HTmin = -1.96°C
Topt = 23.60°C
HTmax = 41.00°C
Hatching Rate (%)
Temperature (°C)

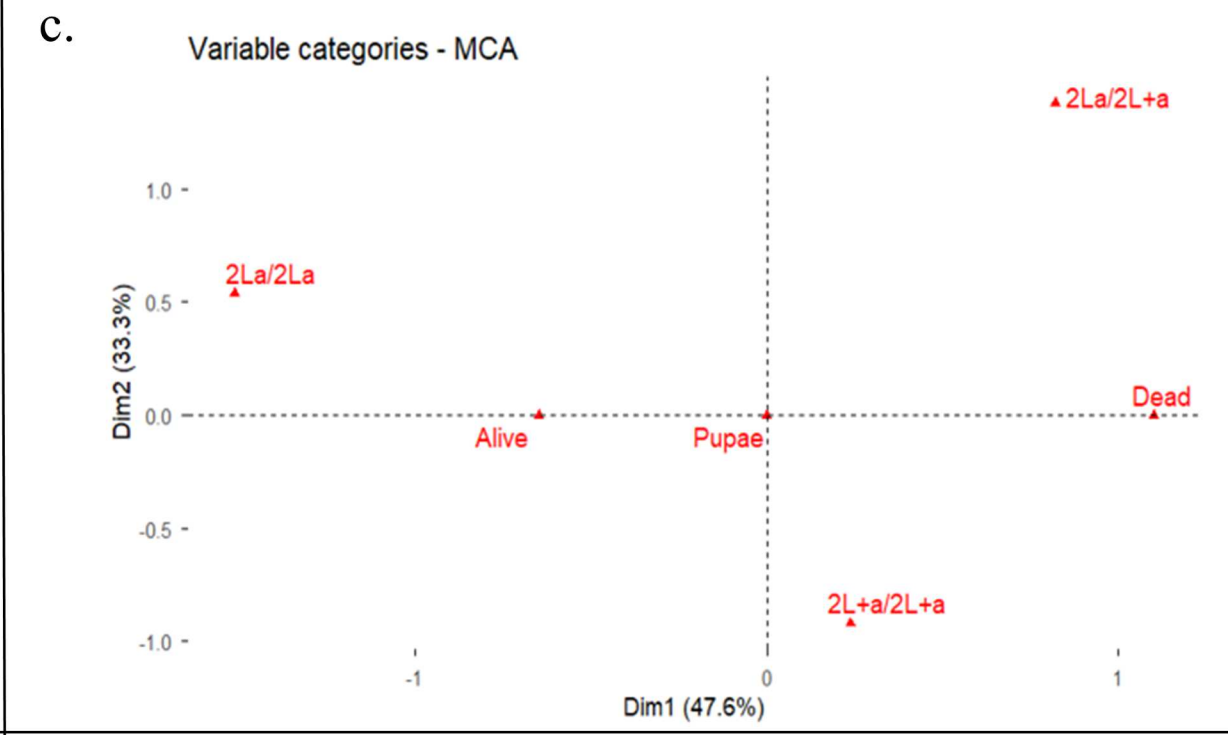

b.
Net Change with Temperature Zones
Population Decline
Population Growth
Cold stress
Optimal range
Heat stress
Net Change (%)
Net Change (%)
Temperature (°C)

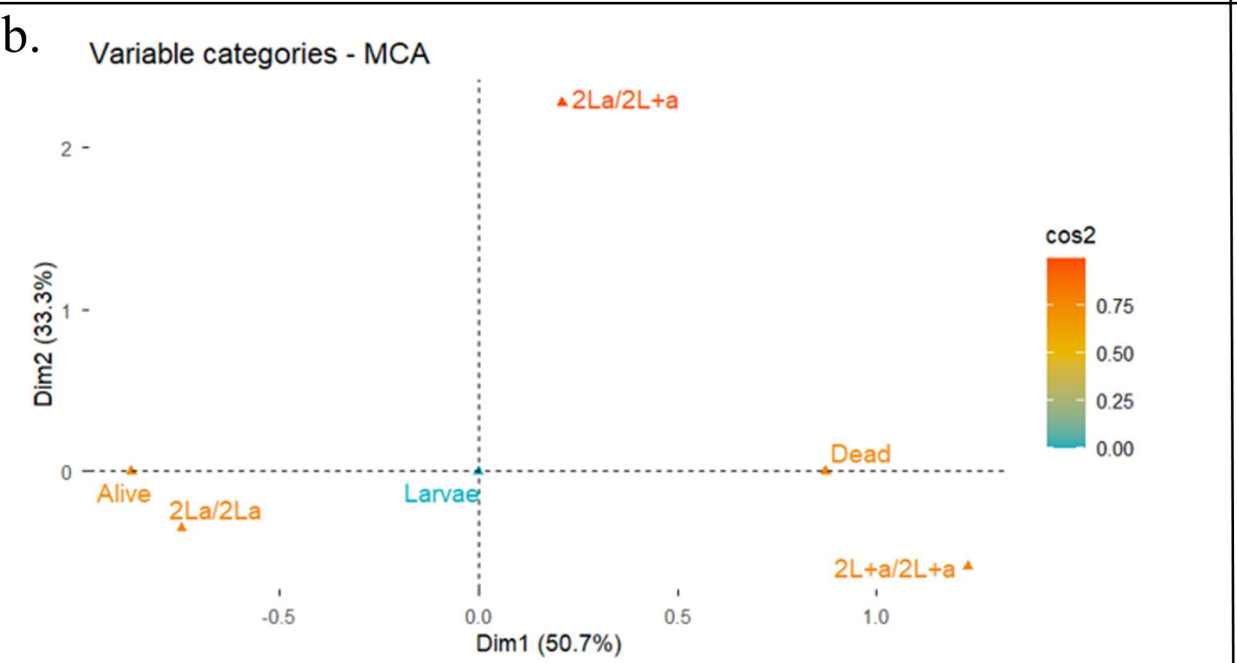

c.
Time (hours)
24 6.7 11.7 10.0 43.3 1.7 8.3 1.7 5.0 8.3 5.0 0.0 0.0 0.0 0.0
48 5.0 8.3 10.0 25.0 26.7 8.3 11.7 11.7 3.3 3.3 0.0 0.0 0.0 0.0
72 1.7 3.3 6.7 8.3 3.3 5.0 6.7 0.0 0.0 0.0 0.0 0.0 0.0 0.0
96 0.0 1.7 5.0 3.3 8.3 3.3 0.0 1.7 0.0 0.0 0.0 0.0 0.0 0.0
120 0.0 0.0 0.0 0.0 6.7 1.7 0.0 0.0 0.0 0.0 1.7 0.0 0.0 0.0
144 0.0 0.0 0.0 0.0 6.7 0.0 0.0 0.0 0.0 0.0 1.7 0.0 0.0 0.0
168 0.0 0.0 0.0 0.0 0.0 0.0 0.0 0.0 0.0 0.0 0.0 0.0 0.0 0.0
0 10 15 25 28 30 32 34 36 38 40 41 42 43
Temperature (°C)
Hatching Rate (%)

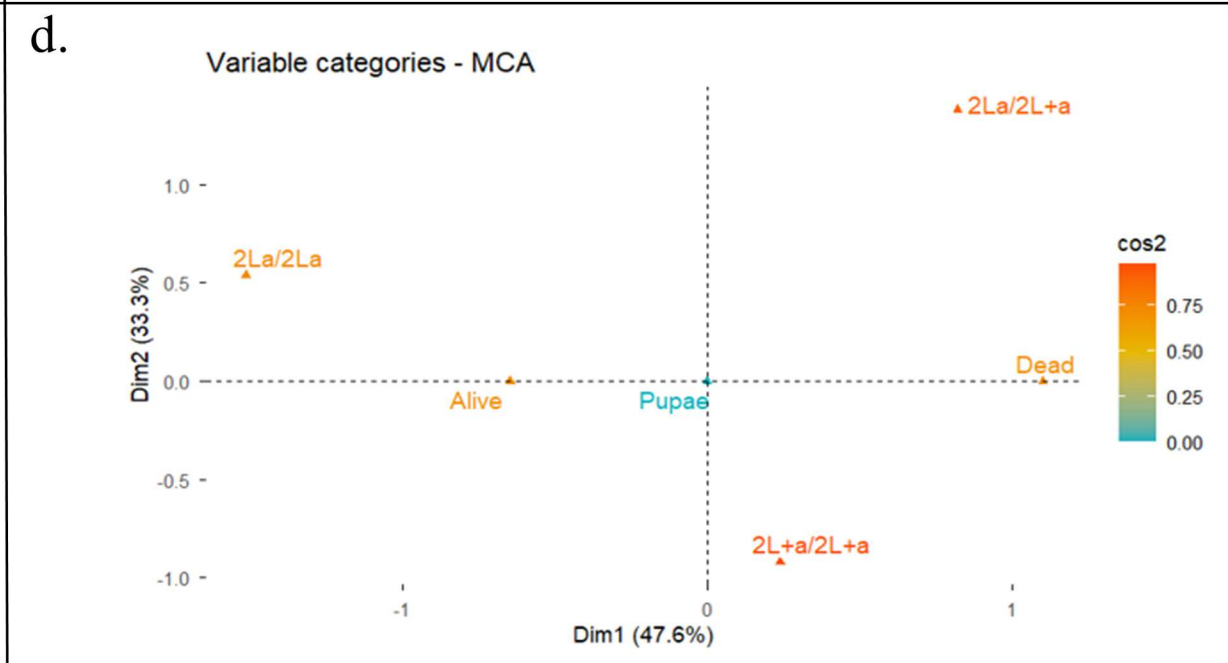

a.
Mortality Rate (%)
Temperature (°C)
Observed Mortality Data
Quadratic Fit (R² = 0.482)
LLT = -5.59°C
Topt = 24.60°C
ULT = 43.00°C
b.
Temperature (°C)
Time (hours)
Larval Mortality Rate (%)
c.
Pupation Rate (%)
Temperature (°C)
Observed Pupation Data
Gaussian Fit (R² = 0.472)
LPTmin = -5.59°C
Topt = 24.73°C
UPTmax = 43.00°C
d.
Temperature (°C)
Time (hours)
Pupation Rate (%)


a.
Observed Mortality Data
Quadratic Fit (R² = 0.376)
LLT = -4.13°C
Topt = 24.41°C
ULT = 43.00°C
Mortality Rate (%)
Temperature (°C)
c.
Observed Emergence Data
Gaussian Fit (R² = 0.365)
LET = -4.13°C
Topt = 24.19°C
UET = 43.00°C
Emergence Rate (%)
Temperature (°C)
b
Temperature (°C)
Time (hours)
Mortality Rate (%)
d.
Temperature (°C)
Time (hours)
Emergence Rate (%)

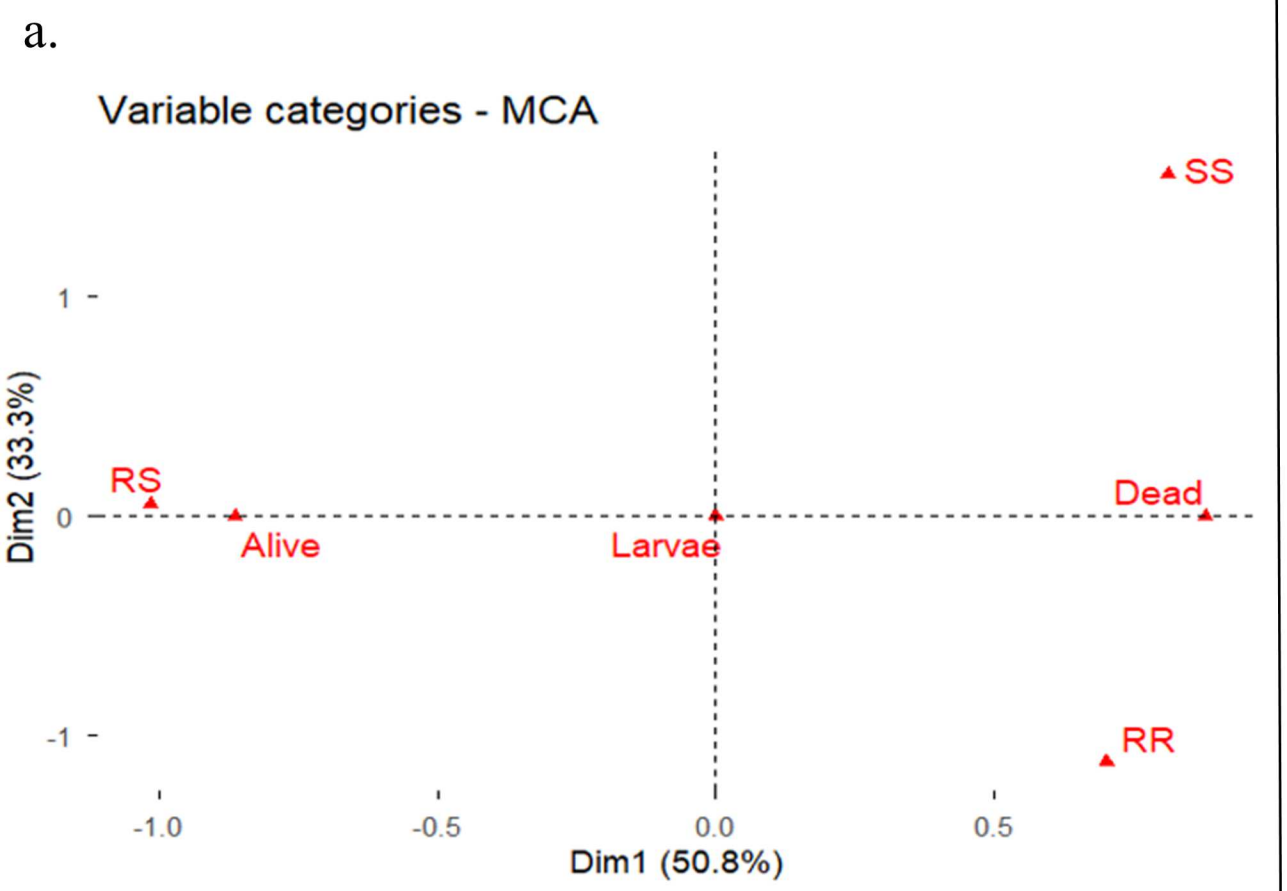

a
Variable categories - MCA
2La/2L+a
Dead
Alive
2La/2La
Larvae
2L+a/2L+a
Dim2 (33.3%)
Dim1 (50.7%)


c.
Variable categories - MCA
2La/2L+a
2La/2La
Dead
Alive
Pupae
2L+a/2L+a
Dim2 (33.3%)
Dim1 (47.6%)

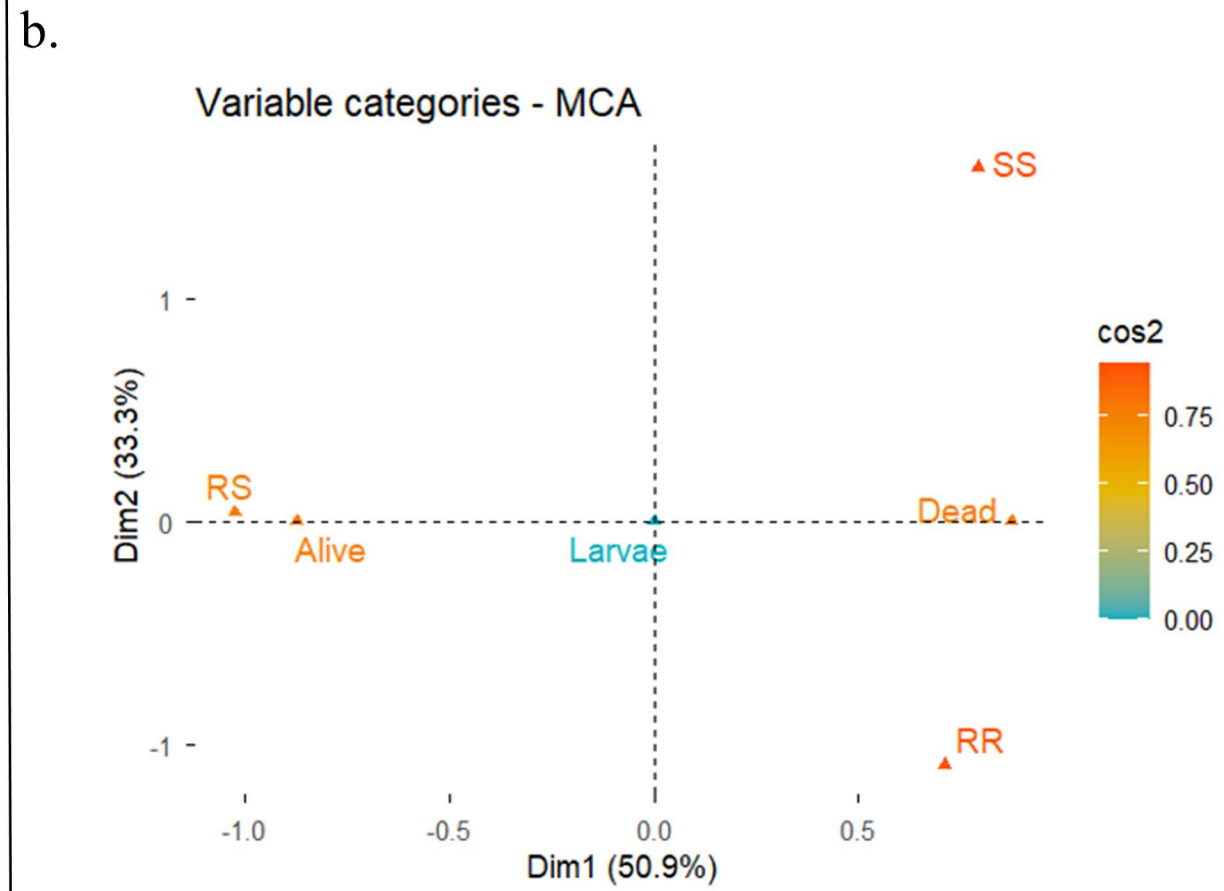

b.
Variable categories - MCA
2La/2L+a
cos2
0.75
0.50
0.25
0.00
Dead
Alive
2La/2La
Larvae
2L+a/2L+a
Dim2 (33.3%)
Dim1 (50.7%)


d.
Variable categories - MCA
2La/2L+a
2La/2La
cos2
0.75
0.50
0.25
0.00
Dead
Alive
Pupae
2L+a/2L+a
Dim2 (33.3%)
Dim1 (47.6%)

a.


Variable categories - MCA
SS
RS
Alive
Larvae
Dead
RR
1
0
-1
-1.0
-0.5
0.0
0.5
Dim2 (33.3%)
Dim1 (50.8%)

b.


Variable categories - MCA
SS
RS
Alive
Larvae
Dead
RR
cos2
0.75
0.50
0.25
0.00
1
0
-1
-1.0
-0.5
0.0
0.5
Dim2 (33.3%)
Dim1 (50.9%)

Supplementary Files

This is a list of supplementary files associated with this preprint. Click to download.

- AdditionalFile1Abdulrahmanetal202607.07.2026.xlsx
- Fig.S1.tif
- Fig.S2.tif
- Fig.S3.tif
- Fig.S4.tif
- Fig.S5.tif
- Fig.S6.tif
- Fig.S7.tif
- Fig.S8.tif
- Fig.S9.tif